

## Discretization error and modelling error in the context of the rapid inflation of hyperelastic membranes

S. SHAW, M.K. WARBY AND J.R. WHITEMAN

*BICOM and Mathematics, Brunel University, Uxbridge, UB8 3PH, UK.*

[Submitted in June 2008]

*This paper is dedicated to A.R. Mitchell, colleague, mentor and friend over many years.*

The computational modelling of the rapid large inflation of hyperelastic circular sheets modelled as axisymmetric membranes is treated, with the aim of estimating engineering quantities of interest and their errors. Fine (involving inertia terms) and coarse (quasi-static) models of the inflation are considered and, using goal oriented techniques, both modelling and discretization error are estimated. Numerical results involving only discretization errors for the quasi-static problem, and both modelling and discretization errors for the dynamic problem are presented.

*Keywords:* finite element method, finite deformation, *a posteriori* modelling error estimates, *a posteriori* discretisation error estimates

### 1. Introduction

The reliability of computed solutions to problems of computational mechanics has in recent years come very much to the fore. The issues involved in this are validation of the mathematical model of the physical event, the verification of the numerical approximation to the solution of the mathematical model, and assessment of the error in the data of the problem which is usually obtained from physical experiments. For a review see e.g. Babuška et al [3]. In this present paper our concern is with the first two of these, estimating approximation error and modelling error, and we shall consider these in the context of the finite inflation of thin sheets modelled as hyperelastic membranes.

The computational modelling of many engineering problems in solid mechanics involves first determining, typically by using finite elements, approximations to a displacement field and possibly also to a velocity field, and then using these to estimate some engineering quantity of interest (QoI). In the case of the inflation of thin sheets, modelled later here as membranes, the QoI may be, for example, the localised stress in part of the sheet, the average thickness over a region, the potential energy of the deformed structure or the kinetic energy associated with the motion. In the assessment of approximation error a numerical scheme will produce a discretisation error, which we can attempt to reduce using expedients such as mesh refinement. The estimation of this type of error and adaptive mesh refinement have been studied extensively over recent years; see for example the books of Ainsworth and Oden [1] and Babuška and Strouboulis [4] for descriptions and assessments of many of the techniques available. Whilst fewer results are available for treating modelling error, extensions of theories related to approximation error have enabled upper and lower bounds of errors in linear functionals of the solutions

to be calculated. These goal oriented methods, such as those produced by Rannacher and his co workers as in [5], Oden and Vemaganti [10], Oden et al. [11], and Oden and Prudhomme [13] and [9], are used in this paper for estimating both discretisation and modelling errors. In the context of the problems that we are considering here it is possible to consider a *fine* problem, based upon the full equations of motion for a rapidly inflating membrane, and also a coarse problem which approximates this but which is formulated in terms of the simpler quasi-static inflation problem. This fine-coarse situation is critical to the machinery which we apply.

The type of problem for which the technique for estimating error can be applied is one which can be described in the following way. The actual problem that we wish to solve, known as the *fine* problem, involves an infinite dimensional function space  $\mathcal{V}$ , a functional  $J : \mathcal{V} \rightarrow \mathbb{R}$ , and a QoI  $J(U)$  where  $U$  satisfies

$$A(U; v) = F(v) \quad \forall v \in \mathcal{V}, \quad (1.1)$$

where  $A(;\cdot)$  is some semilinear form (i.e. linear in arguments to the right of the semi-colon) and  $F(\cdot)$  is a functional. Rarely can  $J(U)$  be determined exactly and instead we obtain an approximation  $u \approx U$ , somehow, and compute  $J(u) \approx J(U)$ . The problem that is used to generate  $u$  is known as the *coarse* approximating problem and typically this problem involves finding  $u$  from an appropriate set such that

$$a(u; v) = F(v) \quad \forall v \in \mathcal{V}_h, \quad (1.2)$$

Typically  $\mathcal{V}_h$  is finite dimensional space (e.g. a finite element space) and the form  $a(;\cdot)$  will be different from  $A(;\cdot)$  in situations when we have modelling error as well as discretization error. As we describe in section 2, to estimate the difference  $J(U) - J(u)$  involves deriving a dual problem from (1.1) which is written in the form: find  $u$  from an appropriate set such that

$$A'(u; v, z) = J'(u; v) \quad \forall v \in \hat{\mathcal{V}}_h \quad (1.3)$$

where  $A'(\cdot; \cdot, \cdot)$  and  $J'(\cdot; \cdot)$  are Gâteaux derivatives of  $A(;\cdot)$  and  $J(\cdot)$  respectively and where  $\hat{\mathcal{V}}_h$  is an appropriate space. The estimate of the error in the QoI is then

$$J(U) - J(u) \approx F(z) - A(u; z). \quad (1.4)$$

Ideally we would like to be able to compute  $u$  and  $J(u)$  with modest computational resources so that

$$|J(U) - J(u)| < \text{required tolerance} \quad (1.5)$$

and if the estimate is good we may nearly achieve this by satisfying

$$|F(z) - A(u; z)| < \text{required tolerance} \quad (1.6)$$

Unfortunately this will often not be possible in situations where we have modelling error, the fine problem is too demanding to tackle and we cannot specify coarse approximating problems which are sufficiently close to the fine problem. In such cases a more realistic aim is to compute  $u$ ,  $J(u)$  and a reasonable estimate of  $|J(U) - J(u)|$  with modest computational resources, i.e. we obtain an estimate  $J(u)$  of  $J(U)$  and an indication as to the magnitude of the error in the estimate.

As we demonstrate later, the complexity of applying this technique to a given situation depends first on the complexity of  $A(;\cdot)$ , from which we get  $A'(\cdot; \cdot, \cdot)$ , and then on the computational effort in solving the dual problem, (1.3). The success (or otherwise) of the procedure

thus depends on the amount of this effort as well as the quality of the estimate (1.4). The degree of success is in general difficult to predict in advance as it can only be guaranteed when  $u$  is sufficiently close to  $U$ . This ‘closeness’ is, in general, not computable.

This paper is organised as follows. In section 2 we give a brief outline of how  $J(U) - J(u)$  can be represented in terms of various candidates for the dual solution in an abstract setting and then, in section 3, we describe the models of membrane inflation in suitable weak forms when we have quasi-static inflation and when we have the full equations of motion. Although obtaining  $A'(\cdot; \cdot, \cdot)$  is straightforward, the details of the dual problem are quite involved. However, these are included here as satisfactorily coping with these details is a significant practical hurdle to overcome in using this methodology. In section 4 we give our numerical scheme for solving the dual problem. Fortunately, for the axisymmetric problem being considered in this paper, we can also attempt to approximately solve the full equations of motion to a high degree of accuracy. This ‘overkill’ solution can then be used as an ‘exact solution’ and employed to test the quality of the estimate. This investigation is outlined in section 5. Finally, in section 6 we give examples demonstrating how the technique works in cases when we only have discretization error, and also when there is both discretization and modelling error.

## 2. Abstract formulation

As described in section 1, an engineering problem is usually posed with some ‘goal’ in mind—the estimation of a physical QoI. Usually the problem is tackled by reducing it (when necessary) to some tractable form (the *modelling approximation*), and then employing some form of simulation (the *discrete approximation*).

In an abstract setting this involves using the solution,  $u$ , to a coarse problem, (1.2), to approximate the solution,  $U$ , to the fine problem, (1.1), and hence estimate the QoI  $J(u) \approx J(U)$ . For the approach adopted here, to estimate the error  $J(U) - J(u)$  involves setting up and solving a dual of the fine problem, (1.3), and then computing an estimate according to (1.4).

In this section we give some details of how these representations and approximations are obtained. Although the technique of estimating error described here can be described briefly, the complexity of actually using it in any particular case depends on the details of  $A(\cdot; \cdot)$  and  $J(\cdot)$  and the success or otherwise in estimating the error accurately with modest computational resources is also highly problem dependent. We first look at representations of the error  $J(U) - J(u)$ .

Let  $w \in \mathcal{V}$  be fixed. The first Gâteaux derivatives of  $J(\cdot)$  and  $A(\cdot; w)$ , in the direction of  $v \in \mathcal{V}$ , are defined respectively by

$$J'(u; v) := \left. \frac{d}{ds} J(u + sv) \right|_{s=0}, \quad A'(u; v, w) := \left. \frac{d}{ds} A(u + sv; w) \right|_{s=0}. \quad (2.1)$$

Higher Gâteaux derivatives can be similarly defined. As with ordinary derivatives of functions of real variables, it then follows that if we let  $e_u = U - u$  and consider the functionals evaluated on  $u + se_u$ ,  $0 \leq s \leq 1$  we then have

$$J(U) - J(u) = \int_0^1 J'(u + se_u; e_u) ds \quad (2.2)$$

and similarly, by (1.1),

$$F(w) - A(u; w) = A(U; w) - A(u; w) = \int_0^1 A'(u + se_u; e_u, w) ds. \quad (2.3)$$

A dual problem and an exact representation of the error  $J(U) - J(u)$  is as follows.

**Dual problem requiring a path from  $u$  to  $U$**

Find  $z \in \mathcal{V}$  such that

$$\int_0^1 A'(u + se_u; v, z) ds = \int_0^1 J'(u + se_u; v) ds \quad \forall v \in \mathcal{V}. \quad (2.4)$$

Then from (2.2) and (2.3) we have

$$J(U) - J(u) = F(z) - A(u; z). \quad (2.5)$$

This is not a computable representation of the error as the problem for  $z$  depends upon the unknown exact solution  $U$ . However, it is a useful starting point from which to derive approximations which can be computed.

**Dual problem when we have an estimate of  $e_u$**

If  $\hat{e}_u \approx e_u$  is available then combining this with a trapezoidal approximation of the integrals in (2.4) and using a finite dimensional space  $\hat{\mathcal{V}}_h \subset \mathcal{V}$  gives the following dual problem. Find  $z \in \hat{\mathcal{V}}_h$  such that

$$A'(u + \hat{e}_u; v, z) + A'(u; v, z) = J'(u + \hat{e}_u; v) + J'(u; v) \quad \text{for all } v \in \hat{\mathcal{V}}_h. \quad (2.6)$$

This produces the estimate,

$$J(U) - J(u) \approx F(z) - A(u; z). \quad (2.7)$$

It should be noted here that if the approximation  $u$  is computed so that  $A(u; v) = F(v)$  for all  $v \in \mathcal{V}_h$  then it is necessary that  $\hat{\mathcal{V}}_h$  is different to  $\mathcal{V}_h$  (which is usually achieved by taking a larger space) as otherwise the right hand side of (2.7) is zero.

**Dual problem only involving  $u$**

If no estimate  $\hat{e}_u$  is available and we only have  $u$  then, by applying the left-hand rectangle rule to (2.4), the simplest dual problem is that of determining  $z \in \hat{\mathcal{V}}_h$  such that

$$A'(u; v, z) = J'(u; v) \quad \text{for all } v \in \hat{\mathcal{V}}_h. \quad (2.8)$$

This gives the estimate

$$J(U) - J(u) \approx F(z) - A(u; z), \quad (2.9)$$

where again  $\hat{\mathcal{V}}_h$  should not be the same as  $\mathcal{V}_h$ .

The accuracy of the estimate in the last case can be obtained more precisely by using Taylor's series with integral forms of the remainder term. We first introduce the intermediate problem: find  $Z \in \mathcal{V}$  such that

$$A'(U; v, Z) = J'(U; v) \quad \forall v \in \mathcal{V}. \quad (2.10)$$

With  $e_u = U - u$ , as before, and with  $e_z = Z - z$ , Oden and Prudhomme in [13] give a representation of the error  $J(U) - J(u)$  of the form

$$J(U) - J(u) = (F(z) - A(u; z)) + (F(e_z) - A(u; e_z)) + \text{smaller terms} \quad (2.11)$$

where the smaller terms involve products of two or more of the errors  $e_u$  and  $e_z$ . We thus need  $e_u$  and  $e_z$  to be 'small' to have a useful result here. For completeness, the precise details can be obtained by first introducing  $g_0 : [0, 1] \rightarrow \mathbb{R}$ ,  $g_1 : [0, 1] \rightarrow \mathbb{R}$ , and  $g_2 : [0, 1] \rightarrow \mathbb{R}$  by

$$g_0(s) = J(u + se_u) + F(z + se_z) - A(u + se_u; z + se_z), \quad (2.12)$$

$$g_1(s) = J'(u + se_u; e_u) - A'(u + se_u; e_u, z + se_z), \quad (2.13)$$

$$g_2(s) = J''(u + se_u; e_u, e_u) - A''(u + se_u; e_u, e_u, z + se_z), \quad (2.14)$$

which, from differentiating with respect to  $s$ , gives

$$g'_0(s) = J'(u + se_u; e_u) + F(e_z) - A'(u + se_u; e_u, z + se_z) - A(u + se_u; e_z) \quad (2.15)$$

$$= g_1(s) + F(e_z) - A(u + se_u; e_z), \quad (2.16)$$

$$g'_1(s) = -A'(u + se_u; e_u, e_z) + J''(u + se_u; e_u, e_u) - A''(u + se_u; e_u, e_u, z + se_z), \quad (2.17)$$

$$= -A'(u + se_u; e_u, e_z) + g_2(s). \quad (2.18)$$

Then observing that

$$g_0(1) = J(U), \quad g_0(0) = J(u) + F(z) - A(u; z) \quad \text{and} \quad g_1(1) = 0, \quad (2.19)$$

we immediately get an expression containing the first term in the error, i.e.

$$J(U) - J(u) = F(z) - A(u; z) + g_0(1) - g_0(0). \quad (2.20)$$

We make use of trapezoidal rule with an integral representation of the error to get an expression for  $g_0(1) - g_0(0)$  as follows.

$$g_0(1) - g_0(0) = \int_0^1 g'_0(s) \, ds = \frac{1}{2}(g'_0(0) + g'_0(1)) + \underbrace{\frac{1}{2} \int_0^1 s(s-1)g_0'''(s) \, ds}_{\text{3rd order in magnitude}}. \quad (2.21)$$

Using  $F(e_z) = A(U; e_z)$ , the connection between  $g'_0$  and  $g_1$ , and also  $g_1(1) = 0$  we have for the first term on the right of this that,

$$g'_0(0) + g'_0(1) = F(e_z) - A(u; e_z) + g_1(0). \quad (2.22)$$

Then, for the term  $g_1(0)$  we have

$$g_1(0) = - \int_0^1 g_1'(s) ds = \int_0^1 A'(u + se_u; e_u, e_z) ds + \int_0^1 g_2(s) ds \quad (2.23)$$

$$= F(e_z) - A(u; e_z) + \underbrace{\int_0^1 g_2(s) ds}_{\text{2nd order in magnitude}}. \quad (2.24)$$

Now for  $0 \leq s \leq 1$ ,  $g_0(s)$  is  $\mathcal{O}(1)$  in magnitude,  $g_0'(s)$  is 1st order in magnitude (as in the expression we have one  $e_u$  term after the semi-colon), and similarly  $g_0''(s)$  is 2nd order in magnitude and  $g_0'''(s)$  is 3rd order in magnitude. We therefore get (2.11) by combining (2.20)–(2.24) and the details confirm that the nearer  $z$  is to the function  $Z$  satisfying (2.10) the better is the computable estimate  $F(z) - A(u; z)$ .

### An overview of the approach

To summarize, to obtain  $u$ ,  $J(u)$  and our estimate of the error in  $J(u)$  requires the following steps.

1. We need  $A(;\cdot)$ ,  $F(\cdot)$  and  $J(\cdot)$ .
2. We determine  $A'(\cdot; \cdot, \cdot)$  and  $J'(\cdot; \cdot)$ .
3. We solve some problem to obtain  $u$ .
4. We solve a dual problem for  $z$  (which depends on  $u$ ).
5. We compute  $J(u)$  and  $F(z) - A(u; z) \approx J(U) - J(u)$ .

As we will see, in the application of the theory to the problem described in section 3 it will also be necessary to express  $A'(\cdot; \cdot, \cdot)$  in a suitable form before the dual problem in step 4 is solved.

### 3. Models for the unconstrained inflation of hyperelastic membranes

The abstract formulation required that the so called “fine model” is expressed in a weak form involving the form  $A(;\cdot)$ . In this section we concentrate on applying this technique to an engineering problem motivated by the thermoforming of thin polymeric sheets. To keep this first attempt as manageable as possible in terms of implementation and experimentation we concentrate on the case of circular sheets with the assumption of axi-symmetry. For more detailed information on this thermoforming problem see, for example, [6, 2, 7, 8].

To test the modelling error estimates the coarse problem will describe the deformation of the sheets in terms of a sequence of static problems. This quasi-static problem corresponds to slowly applied pressure loading and the modelling approximation is that the inertia terms are negligible. The fine problem is then the fully dynamic equations of motion that result when the inertia term is restored. We give examples below of QoI's related to energy and sheet thickness.

On the other hand, to test the discretisation error estimates the fine problem is the quasi-static problem, and the coarse problem is its finite element approximation.

To distinguish the two cases we use the notation  $A_E(;\cdot)$  in the quasi-static equilibrium case and we use again  $A(;\cdot)$  when the full dynamic model is considered. In both cases the unknown is the displacement  $\underline{U}$  at any given position and time. In the simpler quasi-static case the dependence on time  $t$  is only through the time dependent pressure loading and for each fixed time we have equilibrium equations in weak form as,

$$A_E(t)(\underline{U}; \underline{\psi}) = 0 \quad \forall \text{appropriate } \underline{\psi} \in \mathcal{V}, \quad (3.1)$$

where for each  $t \in [0, T]$  considered the domain of  $\underline{U}$  is just a spatial domain,  $\Omega \subset \mathbb{R}^2$ . With pressure loading, the loading term is contained in the expression for  $A_E$ . (In some of what follows we will abbreviate  $A_E(t)(\underline{U}; \underline{\psi})$  to  $A_E(\underline{U}; \underline{\psi})$  when the time  $t$  is clear.)

In the case of the dynamic model the equations of motion involve time derivatives as well as space derivatives and to generate a suitable form for  $A(;\cdot)$  it is convenient to use the approach of Bangerth and Rannacher, [5], who study the wave equation. Hence, we take both the displacement  $\underline{U}$  and the velocity  $\underline{V}$  as unknowns and we impose the condition  $\underline{V} = \dot{\underline{U}}$  weakly. In this way, we have a spatial domain  $\Omega$ , a time interval  $0 \leq t \leq T$ , a space-time region  $Q = \Omega \times [0, T]$  and a problem in weak form as follows.

$$\text{Find } \begin{pmatrix} \underline{U} \\ \underline{V} \end{pmatrix} \in \mathcal{V} \quad \text{such that} \quad A\left(\begin{pmatrix} \underline{U} \\ \underline{V} \end{pmatrix}; \begin{pmatrix} \underline{\psi} \\ \underline{\varrho} \end{pmatrix}\right) = F\left(\begin{pmatrix} \underline{\psi} \\ \underline{\varrho} \end{pmatrix}\right), \quad \forall \text{appropriate } \begin{pmatrix} \underline{\psi} \\ \underline{\varrho} \end{pmatrix} \in \mathcal{V}. \quad (3.2)$$

More concrete details of  $\mathcal{V}$  are given for each of the problems after the expressions for  $A_E(;\cdot)$  and  $A(;\cdot)$  have been derived.

When the fine problem is the quasi-static problem and the coarse solution  $\underline{u}$  is obtained by approximately solving (3.1) by finite elements we have a situation in which we only have discretization error. If we generate an approximate velocity  $\underline{v}$  from  $\underline{u}$  and we use  $(\underline{u}, \underline{v})^T$  as the coarse solution for the dynamic problem (3.2) then we have both modelling error and discretization error.

### 3.1 Expression for $A_E(;\cdot)$ and $A(;\cdot)$

We describe the membrane inflation problem for a hyperelastic axisymmetric circular sheet by first giving the equations for a general three-dimensional body. Then we show how the membrane idealization and the axisymmetry reduce the problem to one in which the unknowns depend only on the radial dimension in a cylindrical polar coordinate system. In our application the undeformed region of our sheet is

$$\Omega_{3D} = \{(r, \vartheta, x_3) : 0 \leq r < 1, -\pi \leq \vartheta < \pi, |x_3| < h_0/2\} \quad (3.3)$$

and this is deformed by a time-dependent pressure  $P(t)$  applied to the lower side of the sheet. Throughout we let  $\Omega$  denote the undeformed mid-surface and for the case above this is just  $\Omega = [0, 1)$  with respect to  $r$ .

**3.1.1 The general 3D case and part of the membrane simplification** If  $\underline{X} \in \Omega_{3D}$  is a general point in the undeformed configuration of the body, with respect to cartesian coordinates with base vectors  $\underline{e}_1, \underline{e}_2, \underline{e}_3$ , then the deformation is described by the mapping

$$\underline{X} \rightarrow \underline{x} := \underline{X} + \underline{U}, \quad (3.4)$$

where  $\underline{U} = \underline{U}(\underline{X})$  is the displacement. The stretching-type quantities that we need are expressed in terms of the deformation gradient

$$\mathbf{F}_{3D} = \mathbf{I}_{3D} + \nabla_{3D}\underline{U}, \quad \text{where } \nabla_{3D}\underline{U} = \left( \frac{\partial U}{\partial X_1}, \frac{\partial U}{\partial X_2}, \frac{\partial U}{\partial X_3} \right). \quad (3.5)$$

For a general deformation  $\mathbf{F}_{3D}$  is  $3 \times 3$ , but one of the membrane simplifications leads to us taking just the first two columns for our membrane deformation gradient:  $\mathbf{F} = (\mathbf{F}_{3D}\underline{e}_1, \mathbf{F}_{3D}\underline{e}_2)$ . This is now described.

One of the properties of the membrane deformation is that material fibres which are normal to the mid-surface at the start of a deformation (i.e. in the  $\underline{e}_3$  direction) remain normal to the sheet throughout the deformation. That is  $\mathbf{F}_{3D}\underline{e}_3$  is in the direction normal to the deformed mid-surface and is orthogonal to  $\mathbf{F}_{3D}\underline{e}_1$  and  $\mathbf{F}_{3D}\underline{e}_2$ . Let  $\mathbf{C} = \mathbf{F}^T\mathbf{F}$  which is  $2 \times 2$  in terms of the components. Then  $\underline{e}_3$  is an eigenvector of  $\mathbf{C}_{3D} = \mathbf{F}_{3D}^T\mathbf{F}_{3D}$  and  $\mathbf{C}$  and  $\mathbf{C}_{3D}$  have the forms

$$\mathbf{C} = \begin{pmatrix} c_{11} & c_{21} \\ c_{21} & c_{22} \end{pmatrix}, \quad \mathbf{C}_{3D} = \begin{pmatrix} c_{11} & c_{21} & 0 \\ c_{21} & c_{22} & 0 \\ 0 & 0 & c_{33} \end{pmatrix}. \quad (3.6)$$

We let  $\underline{c}_1$  and  $\underline{c}_2$  in  $\mathbb{R}^3$  denote unit vectors which are eigenvectors of  $\mathbf{C}_{3D}$  (which are orthogonal to  $\underline{e}_3$ ) with eigenvalues which we denote by  $\lambda_1^2$  and  $\lambda_2^2$  respectively and we let  $\tilde{\underline{c}}_1$  and  $\tilde{\underline{c}}_2$  in  $\mathbb{R}^2$  denote the corresponding eigenvectors of  $\mathbf{C}$ . We let  $\lambda_3^2 = c_{33}$  denote the other eigenvalue of  $\mathbf{C}_{3D}$  and we let

$$\underline{b}_1 = \frac{1}{\lambda_1}\mathbf{F}_{3D}\underline{c}_1, \quad \underline{b}_2 = \frac{1}{\lambda_2}\mathbf{F}_{3D}\underline{c}_2, \quad \underline{n} = \frac{1}{\lambda_3}\mathbf{F}_{3D}\underline{e}_3. \quad (3.7)$$

These vectors are orthonormal eigenvectors of  $\mathbf{B}_{3D} = \mathbf{F}_{3D}\mathbf{F}_{3D}^T$ . Using these eigenvalues and eigenvectors we have the following spectral decompositions and singular valued decompositions.

$$\mathbf{F} = \lambda_1\underline{b}_1\tilde{\underline{c}}_1^T + \lambda_2\underline{b}_2\tilde{\underline{c}}_2^T, \quad (3.8)$$

$$\mathbf{F}_{3D} = \lambda_1\underline{b}_1\underline{c}_1^T + \lambda_2\underline{b}_2\underline{c}_2^T + \lambda_3\underline{n}\underline{e}_3^T, \quad (3.9)$$

$$\mathbf{C} = \lambda_1^2\tilde{\underline{c}}_1\tilde{\underline{c}}_1^T + \lambda_2^2\tilde{\underline{c}}_2\tilde{\underline{c}}_2^T, \quad (3.10)$$

$$\mathbf{C}_{3D} = \lambda_1^2\underline{c}_1\underline{c}_1^T + \lambda_2^2\underline{c}_2\underline{c}_2^T + \lambda_3^2\underline{e}_3\underline{e}_3^T, \quad (3.11)$$

$$\mathbf{B}_{3D} = \lambda_1^2\underline{b}_1\underline{b}_1^T + \lambda_2^2\underline{b}_2\underline{b}_2^T + \lambda_3^2\underline{n}\underline{n}^T. \quad (3.12)$$

In the case of an incompressible deformation which we consider here we have

$$\det \mathbf{F}_{3D} = \lambda_1\lambda_2\lambda_3 = 1. \quad (3.13)$$

The stretching in the elastic body causes stresses which depend on the strain energy function  $W$  of the material (which is introduced properly later) and the stresses can be described using any of the usual stress tensors (see e.g. Ogden in [12]). It is convenient here to describe these tensors using the principal stresses (i.e. eigenvectors) of the Cauchy stress  $\boldsymbol{\sigma}$  as one of the properties of a membrane deformation is that  $\boldsymbol{\sigma}\underline{n} = \underline{0}$ , i.e. one of the principal stresses is 0. For an isotropic elastic material the other directions of principal stress coincide with the directions  $\underline{b}_1$  and  $\underline{b}_2$ , and with  $\sigma_1$  and  $\sigma_2$  denoting the corresponding principal stresses we have the spectral decomposition

$$\boldsymbol{\sigma} = \sigma_1\underline{b}_1\underline{b}_1^T + \sigma_2\underline{b}_2\underline{b}_2^T. \quad (3.14)$$



To describe the equations of motion with respect to the undeformed configuration, instead of the current configuration, we need the nominal stress  $\mathbf{II}_{3D}$  (or equivalently the first Piola stress  $\mathbf{II}_{3D}^T$ ) which is related to  $\boldsymbol{\sigma}$  by

$$\mathbf{II}_{3D} = (\det \mathbf{F}_{3D}) \mathbf{F}_{3D}^{-1} \boldsymbol{\sigma} = \mathbf{F}_{3D}^{-1} \boldsymbol{\sigma}. \quad (3.15)$$

This gives the singular valued decompositions

$$\mathbf{II}_{3D}^T = \frac{\sigma_1}{\lambda_1} \mathbf{b}_1 \tilde{\mathbf{c}}_1^T + \frac{\sigma_2}{\lambda_2} \mathbf{b}_2 \tilde{\mathbf{c}}_2^T, \quad (3.16)$$

$$\mathbf{II}^T = \frac{\sigma_1}{\lambda_1} \mathbf{b}_1 \tilde{\mathbf{c}}_1^T + \frac{\sigma_2}{\lambda_2} \mathbf{b}_2 \tilde{\mathbf{c}}_2^T, \quad (3.17)$$

where here  $\mathbf{II}^T$  is  $3 \times 2$  in shape and is the membrane first Piola stress.

The equations of quasi-static equilibrium in PDE form can be written as

$$\text{Div } \mathbf{II}_{3D} = \underline{\mathbf{0}} \quad \text{where } \text{Div } \mathbf{II}_{3D} = \begin{pmatrix} \frac{\partial \Pi_{11}}{\partial X_1} + \frac{\partial \Pi_{21}}{\partial X_2} + \frac{\partial \Pi_{31}}{\partial X_3} \\ \frac{\partial \Pi_{12}}{\partial X_1} + \frac{\partial \Pi_{22}}{\partial X_2} + \frac{\partial \Pi_{32}}{\partial X_3} \\ \frac{\partial \Pi_{13}}{\partial X_1} + \frac{\partial \Pi_{23}}{\partial X_2} + \frac{\partial \Pi_{33}}{\partial X_3} \end{pmatrix}, \quad (3.18)$$

whereas the dynamics are described by the full equations of motion which, in PDE form, can be written as

$$\rho \dot{\underline{V}} = \text{Div } \mathbf{II}_{3D}, \quad (3.19)$$

$$\underline{V} = \underline{\dot{U}}. \quad (3.20)$$

To get a weak form we take the inner product with  $\underline{\psi}$  in the quasi-static case and with  $(\underline{\psi}, \underline{\theta})^T$  in the dynamic case. In either case, when we derive the expressions we have, when  $\underline{\psi} = \underline{\mathbf{0}}$  on  $\partial\Omega$  and  $d\underline{X} = dX_1 dX_2 dX_3$ ,

$$\int_{\Omega_{3D}} \text{Div } \mathbf{II}_{3D} \cdot \underline{\psi} d\underline{X} \approx -h_0 \iint_{\Omega} \mathbf{II}^T : \nabla \underline{\psi} dX_1 dX_2 + P \iint_{\Omega} \lambda_1 \lambda_2 \underline{n} \cdot \underline{\psi} dX_1 dX_2. \quad (3.21)$$

With clamped boundary conditions this gives us a two-dimensional description in which the unknown displacement field just depends on the position  $(X_1, X_2)$  on the undeformed mid-surface. Also, the pressure traction loading in the full three-dimensional description takes the role of a body type force in this two-dimensional description.

**3.1.2 Simplification in an axisymmetric membrane case** When the undeformed mid-surface of the membrane is, as in (3.3), a circular disk and we use cylindrical polar coordinates,  $(r, \vartheta, x_3)$ , so that an axisymmetric deformation of this mid-surface is described by

$$(r, \vartheta, 0) \rightarrow (r + U_1, \vartheta, U_3), \quad \mathbf{F} = \begin{pmatrix} 1 + U_1' & 0 \\ 0 & 1 + \frac{U_1}{r} \\ U_3' & 0 \end{pmatrix}, \quad (3.22)$$

where ' denotes differentiation with respect to  $r$ . The simplification here is that  $\mathbf{C}$  and  $\mathbf{C}_{3D}$  are both diagonal, the principal stretches are

$$\lambda_1^2 = (1 + U_1')^2 + U_3'^2 \quad \text{and} \quad \lambda_2 = 1 + \frac{U_1}{r} \quad (3.23)$$

corresponding to the directions

$$\underline{t} := \underline{b}_1 = \left( \frac{1+U'_1}{\lambda_1} \right) \underline{e}_r + \left( \frac{U'_3}{\lambda_1} \right) \underline{e}_3 \quad \text{and} \quad \underline{b}_2 = \underline{e}_\vartheta \quad (3.24)$$

with the unit normal  $\underline{n}$  being

$$\underline{n} = - \left( \frac{U'_3}{\lambda_1} \right) \underline{e}_r + \left( \frac{1+U'_1}{\lambda_1} \right) \underline{e}_3. \quad (3.25)$$

The integrals in the weak form involve

$$\tilde{a}_1(\underline{U}; \underline{\psi}) := \mathbf{H}^T : \nabla \underline{\psi} = \Pi_{11} \psi'_1 + \Pi_{13} \psi'_3 + \Pi_{22} \frac{\psi_1}{r} \quad (3.26)$$

$$= \frac{\sigma_1}{\lambda_1^2} ((1+U'_1)\psi'_1 + U'_3\psi'_3) + \frac{\sigma_2}{\lambda_2} \frac{\psi_1}{r}, \quad (3.27)$$

$$\tilde{a}_2(\underline{U}; \underline{\psi}) := \lambda_1 \lambda_2 \underline{n} \cdot \underline{\psi} = \lambda_2 (-U'_3 \psi_1 + (1+U'_1)\psi_3). \quad (3.28)$$

**3.1.3 Material properties and strain energy functions** To complete the mathematical model we need the constitutive relationship between stress and stretch which, in the case of a hyper-elastic material as assumed here, can be expressed in the forms

$$\mathbf{H}^T = \frac{\partial W}{\partial \mathbf{F}}, \quad \text{and in the isotropic case } \sigma_i = \lambda_i \frac{\partial W}{\partial \lambda_i}, \quad i = 1, 2. \quad (3.29)$$

Here  $W$  is the strain energy function for the material being considered as a function  $W = W(\mathbf{F})$  in the first case, and as a function  $W = W(\lambda_1, \lambda_2)$  in the second case. For notational convenience in describing  $A(\cdot; \cdot)$  and for later when describing  $A'(\cdot; \cdot, \cdot)$  we let

$$W_1 := \frac{\partial W}{\partial \lambda_1}, \quad W_2 := \frac{\partial W}{\partial \lambda_2}, \quad W_{11} := \frac{\partial^2 W}{\partial \lambda_1^2}, \quad W_{22} := \frac{\partial^2 W}{\partial \lambda_2^2}, \quad W_{12} = W_{21} := \frac{\partial^2 W}{\partial \lambda_1 \partial \lambda_2}. \quad (3.30)$$

Our expression for  $\tilde{a}_1(\cdot; \cdot)$  becomes

$$\tilde{a}_1(\underline{U}; \underline{\psi}) = \mathbf{H}^T : \nabla \underline{\psi} = \frac{W_1}{\lambda_1} ((1+U'_1)\psi'_1 + U'_3\psi'_3) + W_2 \frac{\psi_1}{r}. \quad (3.31)$$

When we consider the dual problem we need the Gâteaux derivative of this expression and it helps at this stage if we note now that with

$$\lambda_1^2(\underline{U}) = (1+U'_1)^2 + U_3'^2, \quad \lambda_2 = 1 + \frac{U_1}{r} \quad (3.32)$$

we have the Gâteaux derivatives

$$\lambda_1(\underline{U}, \underline{\psi}) \lambda_1'(\underline{U}, \underline{\psi}) = (1+U'_1)\psi'_1 + U_3'\psi'_3, \quad \lambda_2'(\underline{U}, \underline{\psi}) = \frac{\psi_1}{r} \quad (3.33)$$

and hence

$$\tilde{a}_1(\underline{U}; \underline{\psi}) = W_1 \lambda_1'(\underline{U}; \underline{\psi}) + W_2 \lambda_2'(\underline{U}; \underline{\psi}) = W'(\underline{U}; \underline{\psi}), \quad (3.34)$$

where, in the last term,  $W(\underline{U})$  means  $W(\lambda_1(\underline{U}), \lambda_2(\underline{U}))$ .

3.1.4 *The fine problem* With all the terms given and with  $d\underline{X} = r dr$  the quasi-static problem in weak form involves

$$a(\underline{U}; \underline{\psi})_\Omega := h_0 \int_0^1 \mathbf{H}^T : \nabla \underline{\psi} \, r dr - P(t) \int_0^1 \lambda_1 \lambda_2 \underline{n} \cdot \underline{\psi} \, r dr, \quad (3.35)$$

and we have

$$A_E(\underline{U}; \underline{\psi}) = a(\underline{U}; \underline{\psi})_\Omega. \quad (3.36)$$

In the dynamic case the fine problem in weak form similarly involves

$$a(\underline{U}; \underline{\psi})_Q := h_0 \int_0^T \int_0^1 \mathbf{H}^T : \nabla \underline{\psi} \, r dr dt - \int_0^T P(t) \int_0^1 \lambda_1 \lambda_2 \underline{n} \cdot \underline{\psi} \, r dr dt. \quad (3.37)$$

When the initial displacement is  $\underline{U}^0$  and the initial velocity is  $\underline{V}^0$ , and these conditions are imposed weakly, then a weak form of the equations of motion involves finding  $\underline{U}$  and  $\underline{V}$  from appropriate sets such that (1.1) holds for all appropriate test vectors  $\underline{\psi}$  and  $\underline{\theta}$  where

$$\begin{aligned} A\left(\begin{pmatrix} \underline{U} \\ \underline{V} \end{pmatrix}; \begin{pmatrix} \underline{\psi} \\ \underline{\theta} \end{pmatrix}\right) &:= a(\underline{U}; \underline{\psi})_Q + \rho h_0 (\dot{\underline{V}}, \underline{\psi})_Q \\ &\quad + \rho h_0 \left( (\dot{\underline{U}} - \underline{V}, \underline{\theta})_Q + (\underline{U}(\cdot, 0), \underline{\theta})_\Omega + (\underline{V}(\cdot, 0), \underline{\psi})_\Omega \right), \end{aligned} \quad (3.38)$$

$$F\left(\begin{pmatrix} \underline{\psi} \\ \underline{\theta} \end{pmatrix}\right) := \rho h_0 (\underline{U}^0, \underline{\theta})_\Omega + \rho h_0 (\underline{V}^0, \underline{\psi})_\Omega. \quad (3.39)$$

We cannot be completely rigorous here about the function spaces involved for which the problem is properly posed and for which a unique solution exists, these depend on the form of  $W$ , the time range  $[0, T]$  and in more general cases also on the starting shape  $\Omega$  (which is a circular disk here); see [2] for a discussion of these issues. However, throughout we seek a solution to the quasi-static problem with

$$\underline{U}(t) = (U_i(t)), \quad \underline{\psi} = (\psi_i) \quad \text{with } U_i, \psi_i \in H^1(\Omega). \quad (3.40)$$

and for the dynamic case we consider this problem using the same spaces as in [5, p.264], with the unknowns  $\underline{U} = (U_i)$ ,  $\underline{V} = (V_i)$  and test vectors  $\underline{\psi} = (\psi_i)$ ,  $\underline{\theta} = (\theta_i)$  being such that

$$U_i \in H^1((0, T), H^1(\Omega)), \quad V_i \in H^1((0, T), L_2(\Omega)), \quad (3.41)$$

$$\psi_i \in L_2((0, T), H^1(\Omega)), \quad \theta_i \in L_2((0, T), L_2(\Omega)). \quad (3.42)$$

In either case we require that  $U_1(0) = 0$  and that the test space  $\mathcal{V}$  consists of functions  $\underline{\psi}$  which also satisfy the conditions  $\psi_1(0) = \psi_1(1) = \psi_3(1) = 0$ . These deal with axisymmetric condition associated with  $r = 0$  and the Dirichlet boundary conditions at  $r = 1$ .

### 3.2 The Gâteaux derivatives $A'_E(\cdot; \cdot, \cdot)$ and $A'(\cdot; \cdot, \cdot)$

The dual problem that we solve is given in (2.8), and hence requires the Gâteaux derivative of  $A_E(\cdot; \cdot)$  and  $A(\cdot; \cdot)$ . The expressions are only nonlinear in the term involving  $a(\cdot; \cdot)_\Omega$  and

$a(\cdot; \cdot)_Q$  and if we let  $a'(\underline{u}; \underline{\alpha}, \underline{\psi})_\Omega$  and  $a'(\underline{u}; \underline{\alpha}, \underline{\psi})_Q$  denote the Gâteaux derivatives of these in the direction of  $\underline{\alpha}$  then

$$A'_E(\underline{u}; \underline{\alpha}, \underline{\psi}) = a'(\underline{u}; \underline{\alpha}, \underline{\psi})_\Omega, \quad (3.43)$$

$$A'\left(\left(\frac{\underline{u}}{\underline{v}}\right); \left(\frac{\underline{\alpha}}{\underline{\beta}}\right), \left(\frac{\underline{\psi}}{\underline{\theta}}\right)\right) = a'(\underline{u}; \underline{\alpha}, \underline{\psi})_Q + \rho h_0(\dot{\underline{\beta}}, \underline{\psi})_Q \\ + \rho h_0((\dot{\underline{\alpha}} - \underline{\beta}, \underline{\theta})_Q + (\underline{\alpha}(\cdot, 0), \underline{\theta})_\Omega + (\underline{\beta}(\cdot, 0), \underline{\psi})_\Omega) \quad (3.44)$$

$$= a'(\underline{u}; \underline{\alpha}, \underline{\psi})_Q - \rho h_0(\underline{\beta}, \dot{\underline{\psi}})_Q \\ - \rho h_0((\underline{\alpha}, \dot{\underline{\theta}})_Q + (\underline{\beta}, \underline{\theta})_Q - (\underline{\alpha}(\cdot, T), \underline{\theta})_\Omega - (\underline{\beta}(\cdot, T), \underline{\psi})_\Omega). \quad (3.45)$$

Here (3.45) follows from (3.44) by integrating by parts in time and gives us terms evaluated at the final time  $T$ . Note also that (3.45) involves no time derivatives on  $\underline{\alpha}$  and  $\underline{\beta}$  (these have the role of the test functions in the dual problem). Another consequence of writing  $A'$  in this way is that when we consider the problem of determining  $\underline{\psi}$  and  $\underline{\theta}$  such that

$$A'\left(\left(\frac{\underline{u}}{\underline{v}}\right); \left(\frac{\underline{\alpha}}{\underline{\beta}}\right), \left(\frac{\underline{\psi}}{\underline{\theta}}\right)\right) = F\left(\left(\frac{\underline{u}}{\underline{v}}\right); \left(\frac{\underline{\alpha}}{\underline{\beta}}\right)\right) \quad \forall \text{appropriate } \underline{\alpha} \text{ and } \underline{\beta} \quad (3.46)$$

the function spaces can now be such that

$$\psi_i \in H^1((0, T), H^1(\Omega)), \quad \theta_i \in H^1((0, T), L_2(\Omega)), \quad (3.47)$$

$$\alpha_i \in L_2((0, T), H^1(\Omega)), \quad \beta_i \in L_2((0, T), L_2(\Omega)). \quad (3.48)$$

This allows the test functions  $\underline{\alpha}$  and  $\underline{\beta}$  to be discontinuous in time.

To complete the details we still need expressions for

$$a'(\underline{u}; \underline{\alpha}, \underline{\psi})_\Omega = h_0 \int_0^1 \tilde{a}'_1(\underline{u}; \underline{\alpha}, \underline{\psi}) r dr - P(t) \int_0^1 \tilde{a}'_2(\underline{u}; \underline{\alpha}, \underline{\psi}) r dr, \quad (3.49)$$

$$a'(\underline{u}; \underline{\alpha}, \underline{\psi})_Q = h_0 \int_0^T \int_0^1 \tilde{a}'_1(\underline{u}; \underline{\alpha}, \underline{\psi}) r dr dt - \int_0^T P(t) \int_0^1 \tilde{a}'_2(\underline{u}; \underline{\alpha}, \underline{\psi}) r dr dt. \quad (3.50)$$

We obtain  $\tilde{a}'_1(\underline{u}; \underline{\alpha}, \underline{\psi})$  by taking the Gâteaux derivative of  $\tilde{a}_1(\underline{u}; \underline{\psi})$  given in (3.34) to get

$$\tilde{a}'_1(\underline{U}; \underline{\alpha}, \underline{\psi}) = (W_{11} \lambda'_1(\underline{U}; \underline{\alpha}) + W_{12} \lambda'_2(\underline{U}; \underline{\alpha})) \lambda'_1(\underline{U}; \underline{\psi}) + W_1 \lambda''_1(\underline{U}; \underline{\alpha}, \underline{\psi}) \\ + (W_{12} \lambda'_1(\underline{U}; \underline{\alpha}) + W_{22} \lambda'_2(\underline{U}; \underline{\alpha})) \lambda'_2(\underline{U}; \underline{\psi}) + W_2 \lambda''_2(\underline{U}; \underline{\alpha}, \underline{\psi}) \\ = W_{11} \lambda'_1(\underline{U}; \underline{\alpha}) \lambda'_1(\underline{U}; \underline{\psi}) + W_{22} \lambda'_2(\underline{U}; \underline{\alpha}) \lambda'_2(\underline{U}; \underline{\psi}) \\ + W_{12} (\lambda'_1(\underline{U}; \underline{\alpha}) \lambda'_2(\underline{U}; \underline{\psi}) + \lambda'_1(\underline{U}; \underline{\psi}) \lambda'_2(\underline{U}; \underline{\alpha})) \\ + W_1 \lambda''_1(\underline{U}; \underline{\alpha}, \underline{\psi}) + W_2 \lambda''_2(\underline{U}; \underline{\alpha}, \underline{\psi}) \quad (3.51)$$

where the Gâteaux derivatives of the stretch ratios are given by

$$\lambda'_1(\underline{U}; \underline{\psi}) = \frac{(1 + U'_1) \psi'_1 + U'_3 \psi'_3}{\lambda_1}, \quad \lambda'_1(\underline{U}; \underline{\alpha}) = \frac{(1 + U'_1) \alpha'_1 + U'_3 \alpha'_3}{\lambda_1}, \quad (3.52)$$

$$\lambda'_2(\underline{U}; \underline{\psi}) = \frac{\psi_1}{r}, \quad \lambda'_2(\underline{U}; \underline{\alpha}) = \frac{\alpha_1}{r} \quad (3.53)$$

along with

$$\lambda_1''(\underline{U}; \underline{\alpha}, \underline{\psi}) = \frac{\alpha_1' \psi_1' + \alpha_3' \psi_3' - \lambda_1'(\underline{U}; \underline{\alpha}) \lambda_1'(\underline{U}; \underline{\psi})}{\lambda_1} \quad \text{and} \quad \lambda_2''(\underline{U}; \underline{\alpha}, \underline{\psi}) = 0. \quad (3.54)$$

Thus we have

$$a'(\underline{u}; \underline{\alpha}, \underline{\psi})_\Omega = \int_0^1 (\alpha_1, \alpha_1', \alpha_3') G_1 \begin{pmatrix} \psi_1 \\ \psi_1' \\ \psi_3' \end{pmatrix} r dr, \quad a'(\underline{u}; \underline{\alpha}, \underline{\psi})_Q = \int_0^T a'(\underline{u}; \underline{\alpha}, \underline{\psi})_\Omega dt, \quad (3.55)$$

where

$$G_1 = \begin{pmatrix} \frac{W_{22}}{r^2} & \frac{W_{12}(1+U_1')}{r \lambda_1} & \frac{W_{12} U_3'}{r \lambda_1} \\ \frac{W_{12}(1+U_1')}{r \lambda_1} & W_{11} \frac{(1+U_1')^2}{\lambda_1^2} + W_1 \frac{U_3'^2}{\lambda_1^3} & \frac{(1+U_1') U_3'}{\lambda_1^2} \left( W_{11} - \frac{W_1}{\lambda_1} \right) \\ \frac{W_{12} U_3'}{r \lambda_1} & \frac{(1+U_1') U_3'}{\lambda_1^2} \left( W_{11} - \frac{W_1}{\lambda_1} \right) & W_{11} \frac{U_3'^2}{\lambda_1^2} + W_1 \frac{(1+U_1')^2}{\lambda_1^3} \end{pmatrix}. \quad (3.56)$$

By using (3.28) we get the Gâteaux derivative of  $\tilde{a}_2(\underline{u}; \underline{\psi})$  as

$$\tilde{a}_2'(\underline{u}; \underline{\alpha}, \underline{\psi}) = \left( 1 + \frac{u_1}{r} \right) (-\alpha_3' \psi_1 + \alpha_1' \psi_3) + \frac{\alpha_1}{r} (-u_3' \psi_1 + (1 + u_1') \psi_3). \quad (3.57)$$

It is an integral of this that we need and by using integration by parts in the integral involving  $r$  we can write this in a form which only involves  $\alpha_1, \alpha_1', \alpha_3'$  and  $\psi_1, \psi_1', \psi_3'$ , as with the previous term, as follows.

$$r \tilde{a}_2'(\underline{u}; \underline{\alpha}, \underline{\psi}) = ((r + u_1) \alpha_1)' \psi_3 - (r + u_1) \alpha_3' \psi_1 - u_3' \alpha_1 \psi_1. \quad (3.58)$$

Integrating on  $0 \leq r < 1$  and using  $\alpha_1(1) = 0$  gives

$$\int_0^1 \tilde{a}_2'(\underline{u}; \underline{\alpha}, \underline{\psi}) r dr = - \int_0^1 (r + u_1) \alpha_1' \psi_3 + (r + u_1) \alpha_3' \psi_1 + u_3' \alpha_1 \psi_1 r dr \quad (3.59)$$

$$= - \int_0^1 (\alpha_1, \alpha_1', \alpha_3') G_2 \begin{pmatrix} \psi_1 \\ \psi_1' \\ \psi_3' \end{pmatrix} r dr \quad (3.60)$$

where

$$G_2 = \begin{pmatrix} \frac{u_3'}{r} & 0 & \lambda_2 \\ 0 & 0 & 0 \\ \lambda_2 & 0 & 0 \end{pmatrix}. \quad (3.61)$$

### 3.3 $J()$ , $J'(\cdot; \cdot)$ and the dual problem

The quantity of interest estimate, which in the notation of this section is  $J(\underline{u})$  for the quasi-static problem and which is  $J\left(\begin{pmatrix} \underline{u} \\ \underline{v} \end{pmatrix}\right)$  for the dynamic problem, can be quite general with the main requirement being that the dual problems,

$$A'_E(\underline{u}; \underline{\alpha}, \underline{\psi}) = J'(\underline{u}; \underline{\alpha}) \quad \forall \text{ suitable } \underline{\alpha} \quad (3.62)$$

or

$$A'\left(\left(\frac{\underline{u}}{\underline{v}}\right); \left(\frac{\underline{\alpha}}{\underline{\beta}}\right), \left(\frac{\underline{\psi}}{\underline{\theta}}\right)\right) = J'\left(\left(\frac{\underline{u}}{\underline{v}}\right); \left(\frac{\underline{\alpha}}{\underline{\beta}}\right)\right) \quad \forall \text{ suitable } \left(\frac{\underline{\alpha}}{\underline{\beta}}\right) \quad (3.63)$$

that we need to solve are manageable. For the Gâteaux derivative  $J'(\cdot; \cdot)$  to have “matching terms” for  $\underline{\alpha}$  and/or  $\underline{\beta}$  as compared to that which appears in (3.43) or in (3.45) we can have

$$J(\underline{u}) = \int_0^1 r \{\text{expression in } \underline{u}, \underline{u}'\} dr \quad (3.64)$$

in the quasi-static case and

$$J\left(\left(\frac{\underline{u}}{\underline{v}}\right)\right) = \int_0^T \int_0^1 r \{\text{expression in } \underline{u}, \underline{v}, \underline{u}', \underline{v}'\} dr dt \quad (3.65)$$

$$+ \int_0^1 r \{\text{expression in } \underline{u}(\cdot, T), \underline{v}(\cdot, T), \underline{u}'(\cdot, T), \underline{v}'(\cdot, T)\} dr \quad (3.66)$$

in the dynamic case. These leads to a representation of the Gâteaux derivative of the form

$$J'(\underline{u}; \underline{\alpha}) = \int_0^1 (\underline{\alpha} \cdot \underline{J}_\alpha + \underline{\alpha}' \cdot \underline{J}'_\alpha) r dr \quad (3.67)$$

in the quasi-static case and

$$J'\left(\left(\frac{\underline{u}}{\underline{v}}\right); \left(\frac{\underline{\alpha}}{\underline{\beta}}\right)\right) = \int_0^T \int_0^1 (\underline{\alpha} \cdot \underline{J}_\alpha + \underline{\beta} \cdot \underline{J}_\beta + \underline{\alpha}' \cdot \underline{J}'_{\alpha'} + \underline{\beta}' \cdot \underline{J}'_{\beta'}) r dr dt \quad (3.68)$$

$$+ \int_0^1 (\underline{\alpha}(r, T) \cdot \underline{J}_\alpha(r, T) + \underline{\beta}(r, T) \cdot \underline{J}_\beta(r, T) \quad (3.69)$$

$$\underline{\alpha}'(r, T) \cdot \underline{J}'_{\alpha'}(r, T) + \underline{\beta}'(r, T) \cdot \underline{J}'_{\beta'}(r, T)) r dr \quad (3.70)$$

in the dynamic case, where in the above the terms  $\underline{J}_\alpha$ ,  $\underline{J}'_\alpha$ ,  $\underline{J}_\beta$  and  $\underline{J}'_\beta$  provide user-defined data to the dual problem and may depend on  $\underline{u}$  or  $\underline{v}$  (or both). Concrete examples are given later.

The dual problem (3.43) in the quasi-static case is then just a linear problem for  $\underline{\psi}$ . In the dynamic case (3.63) must hold for all  $\underline{\alpha}$  and  $\underline{\beta}$  in the function spaces and the dual problem, which involves finding  $\underline{\psi}$  and  $\underline{\theta}$ , can be broken down into the following parts.

From the terms involving  $\underline{\alpha}(\cdot, T)$  and  $\underline{\beta}(\cdot, T)$  we have the following equations for  $\underline{\psi}(\cdot, T)$  and  $\underline{\theta}(\cdot, T)$ .

$$\rho h_0(\underline{\alpha}(\cdot, T), \underline{\theta}(\cdot, T))_\Omega = \int_0^1 (\underline{\alpha}(r, T) \cdot \underline{J}_\alpha(r, T) + \underline{\alpha}'(r, T) \cdot \underline{J}'_{\alpha'}(r, T)) r dr, \quad (3.71)$$

$$\rho h_0(\underline{\beta}(\cdot, T), \underline{\psi}(\cdot, T))_\Omega = \int_0^1 (\underline{\beta}(r, T) \cdot \underline{J}_\beta(r, T) + \underline{\beta}'(r, T) \cdot \underline{J}'_{\beta'}(r, T)) r dr \quad (3.72)$$

which must hold for all suitable  $\underline{\alpha}(r, T)$  and  $\underline{\beta}(r, T)$ . From the term involving  $\underline{\beta}(r, t)$  for  $0 \leq t < T$  we get

$$-\rho h_0(\underline{\psi} + \underline{\theta}, \underline{\beta})_Q = \int_0^T \int_0^1 (\underline{\beta} \cdot \underline{J}_\beta + \underline{\beta}' \cdot \underline{J}'_{\beta'}) r dr dt. \quad (3.73)$$

Similarly, considering the  $\underline{\alpha}(r, t)$  terms for  $0 \leq t < T$  we get

$$a'(\underline{U}; \underline{\alpha}, \underline{\psi})_Q - \rho h_0(\underline{\alpha}, \dot{\underline{\theta}})_Q = \int_0^T \int_0^1 (\underline{\alpha} \cdot \underline{J}_{\alpha} + \underline{\alpha}' \cdot \underline{J}_{\alpha'}) r dr dt. \quad (3.74)$$

The equations (3.71), (3.72), (3.73) and (3.74) give a linear dual problem for  $\underline{\psi}$  and  $\underline{\theta}$ . This has a structure similar to the problem of solving the equations of motion to determine the displacement  $\underline{U}$  and the velocity  $\underline{V}$ , with the main difference being that for the dual problem we have final time conditions (i.e. at  $t = T$ ) instead of initial conditions. Equation (3.73) is similar to the condition  $\underline{\dot{U}} = \underline{V}$ , which is imposed weakly, in that it connects  $\underline{\dot{\psi}}$  and  $\underline{\dot{\theta}}$ . Equation (3.74) involves the term  $a'(\cdot; \cdot, \cdot)_Q$  which is encountered in numerical schemes for approximately solving the fine problem for  $\underline{U}$  and  $\underline{V}$  by using a Newton iteration.

#### 4. Computational details for solving the dual problem

In section 2 we listed the steps required to get the estimate of the error in the QoI with the main ones being obtaining the coarse and dual solutions. In this section we consider what this involves for the membrane inflation problem.

##### 4.1 The quasi-static case

When the problem that we want to solve corresponds to (3.1) with  $A_E$  given in (3.36) then we use a standard finite element procedure involving a piecewise polynomial finite element space  $\mathcal{V}_h \subset (H_1(\Omega))^2$  to generate a coarse solution  $\underline{u}$  with  $\underline{u} - \underline{u}(t_0) \in \mathcal{V}_h$  such that

$$a(t)(\underline{u}; \underline{\psi})_{\Omega} = 0 \quad \forall \underline{\psi} \in \mathcal{V}_h. \quad (4.1)$$

Here  $\underline{u}(t_0)$  is the initial displacement which will be non-zero if the inflation is started from a pre-stretched state. Equation (4.1) is a nonlinear problem which we can attempt to solve using Newton's method at each fixed time that we consider. Specifically, if we have solved the problem at times  $0 = t_0 < t_1 < t_2 < \dots < t_{j-1}$  with solutions  $\underline{u}(t_0), \underline{u}(t_1), \dots, \underline{u}(t_{j-1})$  then we can attempt to get the solution at time  $t_j$  by the following algorithm.

Set  $\underline{u}^{(0)} = \underline{u}(t_{j-1})$ .

For  $k = 1, 2, \dots$

Solve for  $\underline{\delta}^{(k)}$

$$a(t_j)(\underline{u}^{(k-1)}; \underline{\psi})_{\Omega} + a'(t_j)(\underline{u}^{(k-1)}; \underline{\delta}^{(k)}, \underline{\psi})_{\Omega} = 0 \quad \forall \underline{\psi} \in \mathcal{V}_h, \quad (4.2)$$

Set  $\underline{u}^{(k)} = \underline{u}^{(k-1)} + \underline{\delta}^{(k)}$ .

As  $a'(t_j)(\cdot; \cdot, \cdot)_{\Omega}$  is symmetric in the 2 arguments following the semi-colon in this application this leads to a sparse and symmetric linear system at each stage in order to obtain the nodal values of  $\underline{\delta}^{(k)} = \underline{u}^{(k)} - \underline{u}^{(k-1)}$ .

If the QoI involves  $\underline{u}(t_j)$  then the dual problem that we need to construct and solve involves a similar set-up in that we seek  $\underline{\psi}(t_j) \in \hat{\mathcal{V}}_h$  such that

$$a'(t_j)(\underline{u}(t_j); \underline{\alpha}, \underline{\psi}(t_j))_{\Omega} = J'(\underline{u}(t_j); \underline{\alpha}) \quad \forall \underline{\alpha} \in \hat{\mathcal{V}}_h. \quad (4.3)$$

(Here  $\underline{\psi}(t_j)$  is shorthand for the function  $\underline{\psi}(\cdot, t_j)$ .) The similarity between (4.2) and (4.3) is that we have the same  $a'(t_j)(\cdot; \cdot, \cdot)_{\Omega}$  expression which thus leads to a linear system which is sparse and symmetric for the nodal values of  $\underline{\psi}(t_j)$ . However there are crucial differences as the spaces  $\mathcal{V}_h$  and  $\hat{\mathcal{V}}_h$  are different and, following a previous comment, we choose  $\hat{\mathcal{V}}_h$  so that  $\mathcal{V}_h \subset \hat{\mathcal{V}}_h$ . That is we solve for a function  $\underline{\psi}(t_j)$  from a space  $\hat{\mathcal{V}}_h$  using data (the function  $\underline{u}(\cdot, t_j)$ ) defined on a different space  $\mathcal{V}_h$ . This feature of needing two different spaces at the same time makes the implementation of (4.3) more challenging than the implementation of (4.2).

#### 4.2 The dynamic case

When the problem that we want to solve is the full equations of motion corresponding to (3.2) with  $A(\cdot; \cdot)$  and  $F(\cdot)$  given in (3.38) and (3.39), the additional effort in obtaining a dual solution first involves setting up a space-time mesh of  $Q$  involving time levels  $0 = t_0 < t_1 < \dots < t_N = T$ . The unknowns in the dual problem in this case are  $\underline{\psi}(r, t)$  and  $\underline{\theta}(r, t)$ . If the spatial discretization is fixed in time and leads to the basis functions  $\bar{H}_1(r), \dots, \bar{H}_M(r)$  then we define the approximation such that on a time level

$$\underline{\psi}(r, t_j) := \underline{\psi}^j(r) := \sum_{i=1}^M \underline{\psi}_i^j H_i(r), \quad \underline{\theta}(r, t_j) := \underline{\theta}^j(r) := \sum_{i=1}^M \underline{\theta}_i^j H_i(r), \quad (4.4)$$

where  $\underline{\psi}_i^j$  and  $\underline{\theta}_i^j$  denote the nodal values, and between time levels, i.e.  $t_{j-1} < t < t_j$  we have

$$\underline{\psi}(r, t) = \left( \frac{t_j - t}{t_j - t_{j-1}} \right) \underline{\psi}^{j-1}(r) + \left( \frac{t - t_{j-1}}{t_j - t_{j-1}} \right) \underline{\psi}^j(r), \quad (4.5)$$

$$\underline{\theta}(r, t) = \left( \frac{t_j - t}{t_j - t_{j-1}} \right) \underline{\theta}^{j-1}(r) + \left( \frac{t - t_{j-1}}{t_j - t_{j-1}} \right) \underline{\theta}^j(r). \quad (4.6)$$

In this way we satisfy the requirement that

$$\psi_i \in H^1((0, T), H^1(\Omega)), \quad \theta_i \in H^1((0, T), L_2(\Omega)). \quad (4.7)$$

For the test functions  $\underline{\alpha} = (\alpha_i)$  and  $\underline{\beta} = (\beta_i)$  we take functions which satisfy

$$\alpha_i \in L_2((0, T), H^1(\Omega)), \quad \beta_i \in L_2((0, T), H^1(\Omega)) \quad (4.8)$$

and specifically use functions which are piecewise constant in time such that when  $t_{j-1} < t < t_j$  the span of the functions for  $\underline{\alpha}$  and for  $\underline{\beta}$  corresponds to

$$\text{span} \left\{ \begin{pmatrix} H_1(r) \\ 0 \end{pmatrix}, \begin{pmatrix} 0 \\ H_1(r) \end{pmatrix}, \dots, \begin{pmatrix} H_M(r) \\ 0 \end{pmatrix}, \begin{pmatrix} 0 \\ H_M(r) \end{pmatrix} \right\}. \quad (4.9)$$

We also use this space for the test functions  $\underline{\alpha}(r, T)$  and  $\underline{\beta}(r, T)$  needed in the approximate solution of (3.71) and (3.72) to get  $\underline{\psi}(r, T)$  and  $\underline{\theta}(r, T)$ . Once the final time values are obtained we then approximately solve (3.73) and (3.74) for  $j = N - 1, N - 2, \dots, 1, 0$  as follows.

On each time interval  $(t_j, t_{j+1})$  the time dependence of each term we need to consider is constant or linear in  $t$  and hence all the time integrations can be done exactly. Thus when the



solution at time  $t_{j+1}$  is known we can approximately solve (3.73) to generate a function  $\underline{\gamma}^j(r, t)$  such that

$$\underline{\psi}^{j+1} - \underline{\psi}^j + \frac{1}{2}(\underline{\theta}^j + \underline{\theta}^{j+1}) = \underline{\gamma}^j \quad (4.10)$$

leading to

$$\dot{\underline{\theta}} = \frac{\underline{\theta}^{j+1} - \underline{\theta}^j}{t_{j+1} - t_j} = 2 \frac{(\underline{\psi}^{j+1} - \underline{\psi}^j + \underline{\theta}^{j+1} - \underline{\gamma}^j)}{t_{j+1} - t_j}. \quad (4.11)$$

Substituting this into (3.74) gives a linear problem for the unknown  $\underline{\psi}^j(r)$ . Again, as in the quasi-static case, a challenging aspect in implementing this procedure is that the problem that we must solve to get  $\underline{\psi}^j$  involves, as data, a previously computed displacement field  $\underline{u}$  defined on a different space-time mesh to that being used to obtain  $\underline{\psi}$  and  $\underline{\theta}$ .

## 5. Other computational details

So far we have given an overview in section 2 of the procedure for approximately (in terms of modelling and discretisation) solving a problem and of estimating the error in a quantity of interest. We then specialised to the case where the problem is one of membrane inflation.

There are some additional computational steps which we can also take as it is possible, in this case, to attempt to approximately solve the full equations of motion to a high degree of accuracy. This produces a numerical solution which can play the role of an exact solution and can therefore be used to check the accuracy of the estimates. It is also possible in the quasi-static case, when we only have discretization error, to adaptively refine the mesh to actually achieve (1.5). We describe briefly both of these cases next.

### 5.1 Quasi-static problem: when we only have discretization error

When the fine problem is given by (3.1), our approximate displacement  $\underline{u} = \underline{u}_h$  with  $\underline{u} - \underline{u}(t_0) \in \mathcal{V}_h$  and the aim is to get a dual solution using the space  $\hat{\mathcal{V}}_h$  with  $\mathcal{V}_h \subset \hat{\mathcal{V}}_h$  we can also use the larger space  $\hat{\mathcal{V}}_h$  to estimate the error  $\underline{e} = \underline{U} - \underline{u}_h$ . This can be done by noting that

$$0 = A_E(\underline{U}; \underline{\psi}) = A_E(\underline{u}_h + \underline{e}; \underline{\psi}) = A_E(\underline{u}_h; \underline{\psi}) + A'_E(\underline{u}_h; \underline{e}, \underline{\psi}) + \text{higher order terms} \quad (5.1)$$

and thus we get an estimate  $\hat{\underline{e}} \in \hat{\mathcal{V}}_h$  of  $\underline{e}$  by solving

$$A'_E(\underline{u}_h; \hat{\underline{e}}, \underline{\psi}) = -A_E(\underline{u}_h; \underline{\psi}) \quad \forall \underline{\psi} \in \hat{\mathcal{V}}_h. \quad (5.2)$$

Following (2.6) and (2.7) we can take the dual problem for  $\underline{\psi} \in \hat{\mathcal{V}}_h$  to be

$$A'_E(\underline{u} + \hat{\underline{e}}; \underline{\alpha}, \underline{\psi}) + A'_E(\underline{u}; \underline{e}, \underline{\psi}) = J'(\underline{u} + \hat{\underline{e}}; \underline{\alpha}) + J'(\underline{u}; \underline{\alpha}) \quad \text{for all } \underline{\alpha} \in \hat{\mathcal{V}}_h \quad (5.3)$$

leading to the estimate

$$J(\underline{U}) - J(\underline{u}) \approx -A_E(\underline{u}; \underline{\psi}) = -a(\underline{u}; \underline{\psi})_\Omega \quad (5.4)$$

using (3.36). If  $\underline{u}$  is obtained using a mesh of  $m$  non-overlapping elements occupying  $\Omega_1, \dots, \Omega_m$  and if  $\underline{\psi}_I \in \mathcal{V}_h$  is the nodal interpolant of  $\underline{\psi} \in \hat{\mathcal{V}}_h$  then

$$a(\underline{u}; \underline{\psi})_\Omega = a(\underline{u}; \underline{\psi} - \underline{\psi}_I)_\Omega = \sum_{k=1}^m a(\underline{u}; \underline{\psi} - \underline{\psi}_I)_{\Omega_k}. \quad (5.5)$$

It is also worth noting here that by writing  $\underline{u} = \underline{U} - \underline{e}$  where, as before,  $\underline{U}$  is the exact solution and  $\underline{e}$  is the error, we can also write

$$a(\underline{u}; \underline{\psi} - \underline{\psi}_I)_\Omega = a(\underline{U} - \underline{e}; \underline{\psi} - \underline{\psi}_I)_\Omega = -a'(\underline{U}; \underline{e}, \underline{\psi} - \underline{\psi}_I)_\Omega + \text{higher order terms.} \quad (5.6)$$

The order of magnitude of  $J(\underline{U}) - J(\underline{u})$  in terms of powers of the mesh size  $h$  used to obtain  $\underline{u}$  is hence the product of the order of magnitude of the error  $\underline{e} = \underline{U} - \underline{u}$  and the interpolation error  $\underline{\psi} - \underline{\psi}_I$ , where in both cases the precise details involve the first spatial derivatives of these quantities. Hence, if degree  $p$  polynomials are used and  $J$  is such that the dual solution  $\underline{\psi}$  is sufficiently smooth then both the terms give order  $h^p$  quantities leading to  $J(\underline{U}) - J(\underline{u})$  being of order  $h^{2p}$ . We make use of this observation to determine how to refine the mesh in an economical way in order to compute  $J(\underline{u}) = J(\underline{u}_h)$  so that  $|J(\underline{U}) - J(\underline{u}_h)| < \text{tol}$ . In terms of the mesh itself we would like a mesh for which

$$\left| a(\underline{u}; \underline{\psi} - \underline{\psi}_I)_{\Omega_k} \right| \approx \frac{\text{tol}}{m}, \quad k = 1, 2, \dots, m. \quad (5.7)$$

If the element quantity for the  $k$ th element is larger than  $\text{tol}/m$  then we opt to refine the  $k$ th element. If we are using degree  $p$  polynomials then the previous comments indicate that dividing the element into  $q_k$  equal parts should decrease the quantity corresponding to the region of the  $k$ th element by a factor of about  $q_k^{2p}$ . This suggests that we select  $q_k$  so that

$$q_k^{2p} \approx \frac{\left| a(\underline{u}_h, \underline{\psi} - \underline{\psi}_I)_{\Omega_k} \right|}{\text{tol}/m} > 1. \quad (5.8)$$

In fact it is usually beneficial to take a slightly larger value than this as otherwise a strategy of aiming to almost exactly get to the required accuracy often results in a new mesh that produces an error slightly larger than  $\text{tol}$ . If the value obtained for  $q_k$  selected by the above is large then it is also beneficial to reduce it to some chosen fixed value (we use 16 below) with the knock on effect that more than one mesh refinement will be needed before the accuracy of  $\text{tol}$  is obtained.

The mesh adaption procedure used is as follows.

1. We solve on a mesh of  $m$  elements and compute the quantities  $a(\underline{u}_h, \underline{\psi} - \underline{\psi}_I)_{\Omega_k}$ ,  $k = 1, 2, \dots, m$ .

2. If

$$\left| \sum_{k=1}^m a(\underline{u}_h, \underline{\psi} - \underline{\psi}_I)_{\Omega_k} \right| \leq \text{tol} \quad (5.9)$$

then we stop the computation.

3. For  $k = 1, 2, \dots, m$  we test as follows.

If

$$\left| a(\underline{u}_h, \underline{\psi} - \underline{\psi}_I)_{\Omega_k} \right| < \frac{\text{tol}}{m} \quad (5.10)$$

then we set  $q_k = 1$  and goto the next value of  $k$ .

Otherwise we compute

$$q_k = \text{ceil} \left( \frac{1.05 |a(\underline{u}_h, \underline{\psi} - \underline{\psi}_I)_{\Omega_k}|}{\text{tol}/m} \right)^{1/(2p)}. \quad (5.11)$$

If  $q_k > 16$  then we re-set  $q_k = 16$ .

We divide the  $k$ th element into  $q_k$  parts.

4. We replace  $m$  by  $q_1 + q_2 + \dots + q_m$  and goto step 1.

The factor of 1.05 and the bound of 16 used above were selected based on our experience with the computational results. These values work reasonably well in the test problems considered although other values close to these are also likely to work well.

## 5.2 Dynamic problem: numerical procedure

To approximately solve the full equations of motion by finite elements we need a space-time mesh of  $Q = \Omega \times [0, T]$ . If  $0 = t_0 < t_1 < \dots < t_N = T$  denote the time levels then, as in the description given in section 4.2, we take approximations at each time level  $t_j$  of the form

$$\underline{u}(r, t_j) := \underline{u}^j(r) := \sum_{i=1}^M \underline{u}_i^j H_i(r), \quad \underline{v}(r, t_j) := \underline{v}^j(r) := \sum_{i=1}^M \underline{v}_i^j H_i(r), \quad (5.12)$$

where  $\underline{u}_i^j$  and  $\underline{v}_i^j$  denote the nodal values and where  $H_1(r), \dots, H_M(r)$  denote the spatial basis functions. For  $t_{j-1} < t < t_j$  we have

$$\underline{u}(r, t) = \left( \frac{t_j - t}{t_j - t_{j-1}} \right) \underline{u}^{j-1}(r) + \left( \frac{t - t_{j-1}}{t_j - t_{j-1}} \right) \underline{u}^j(r), \quad (5.13)$$

$$\underline{v}(r, t) = \left( \frac{t_j - t}{t_j - t_{j-1}} \right) \underline{v}^{j-1}(r) + \left( \frac{t - t_{j-1}}{t_j - t_{j-1}} \right) \underline{v}^j(r). \quad (5.14)$$

To start the procedure we obtain  $\underline{u}^0(r)$  and  $\underline{v}^0(r)$  by solving

$$\int_0^1 \underline{u}^0(r) \cdot \underline{\theta} r dr = \int_0^1 \underline{U}^0(r) \cdot \underline{\theta} r dr, \quad \int_0^1 \underline{v}^0(r) \cdot \underline{\psi} r dr = \int_0^1 \underline{V}^0(r) \cdot \underline{\psi} r dr \quad \forall \underline{\psi}, \underline{\theta} \in \mathcal{S}_h \quad (5.15)$$

where

$$\mathcal{S}_h = \text{span} \left\{ \begin{pmatrix} H_i(r) \\ 0 \end{pmatrix}, \begin{pmatrix} 0 \\ H_i(r) \end{pmatrix} : i = 1, 2, \dots, M \right\}. \quad (5.16)$$

If the problem has been solved at times  $t_0 < t_1 < \dots < t_{j-1}$  and the solution is sought at time  $t_j$  then

$$\int_{t_{j-1}}^{t_j} \int_0^1 \rho h_0 (\dot{\underline{u}} - \underline{v}) \cdot \underline{\theta} r dr dt = 0 \quad \forall \underline{\theta} \in \mathcal{S}_h \quad (5.17)$$

leads to

$$\underline{u}^j - \underline{u}^{j-1} = \frac{1}{2} (t_j - t_{j-1}) (\underline{v}^{j-1} + \underline{v}^j) \quad (5.18)$$

so that the acceleration term is given by

$$\frac{\underline{v}^j - \underline{v}^{j-1}}{t_j - t_{j-1}} = \frac{2}{t_j - t_{j-1}} \left( \frac{\underline{u}^j - \underline{u}^{j-1}}{t_j - t_{j-1}} - \underline{v}^{j-1} \right). \quad (5.19)$$

By defining  $\underline{u}^{j-1/2} = (\underline{u}^{j-1} + \underline{u}^j)/2$  the problem for determining  $\underline{u}^j$  involves solving the nonlinear problem

$$\int_0^1 \left\{ \tilde{a}_1(\underline{u}^{j-1/2}; \underline{\psi}) - P(t_{j-1/2}) \tilde{a}_2(\underline{u}^{j-1/2}; \underline{\psi}) + \frac{2\rho h_0}{t_j - t_{j-1}} \left( \frac{\underline{u}^j - \underline{u}^{j-1}}{t_j - t_{j-1}} - \underline{v}^{j-1} \right) \cdot \underline{\psi} \right\} r dr = 0, \quad \forall \underline{\psi} \in \mathcal{S}_h. \quad (5.20)$$

## 6. Numerical Examples

As we touched on earlier, how well the technique described above works for accurately estimating the error in the approximation of a quantity of interest is highly problem dependent. In particular it is not always clear in advance when the procedure will work well and when it will work less well. We illustrate this here with a number of examples involving both ‘easier’ cases—a quasi-static fine model and only discretization error in the coarse model—and ‘harder’ cases—involving the full equations of motion, modelling error and a dual solution which is highly oscillatory.

### 6.1 The quasi-static problem – discretization only

We first consider the quasi-static inflation problem for a strain energy function  $W$  of the Mooney-Rivlin form given by

$$W = \frac{1}{2} (\lambda_1^2 + \lambda_2^2 + \lambda_3^2 - 3) + \frac{0.1}{2} (\lambda_1^{-2} + \lambda_2^{-2} + \lambda_3^{-2} - 3) \quad (6.1)$$

where, as before,  $\lambda_1$  and  $\lambda_2$  are the principal stretch ratios tangential to the mid-surface and where  $\lambda_3 = 1/(\lambda_1\lambda_2)$  is the stretch ratio through the thickness. The deformed membrane profiles that are obtained only depend on the ratio  $P/h_0$ , where  $P$  is the applied pressure and  $h_0$  is the undeformed thickness. The profiles obtained and the paths of selected points as the pressure is increased are shown in figure 6.1. The profiles suggest that the solution is “smooth”, high accuracy is likely to be attainable and that the error estimation technique should do well. This is exactly what we observe in the case of the following two quantities of interest,

$$J_1(\underline{U}) = \int_0^1 h_0 r W - \frac{P}{3} (r + U_1) (-(r + U_1) U_3' + (1 + U_1') U_3) dr, \quad (6.2)$$

$$= \int_0^1 h_0 r W - P (r + U_1) (1 + U_1') U_3 dr, \quad (6.3)$$

which is the total potential energy, and

$$J_2(\underline{U}) = \frac{2}{b^2} \int_0^b r \lambda_3(r) dr \quad (6.4)$$

which is a measure of the thickness ratio  $\lambda_3$  in the vicinity of the pole at  $r = 0$ .

We take  $b = 1/8$  in the computations and ensure that  $r = b$  is a node on each of the meshes used. In the  $J_1$  expression we set  $h_0 = 1$ ,  $P = 3$ . In the expression for  $J_1$  and  $J_2$  the displacement  $\underline{U}$  is the displacement corresponding to these values, i.e. the displacement corresponds to the outermost profile shown in figure 6.1. The first Gâteaux derivatives of  $J_1$  and  $J_2$  are straightforward to get. From (6.3) we get

$$J'_1(\underline{U}; \underline{\alpha}) = \int_0^1 h_0 r W'(\underline{U}; \underline{\alpha}) - P((r + U_1)\alpha_1)'U_3 + (r + U_1)(1 + U_1')\alpha_3 \, dr, \quad (6.5)$$

$$= \int_0^1 h_0 r W'(\underline{U}; \underline{\alpha}) + P((r + U_1)\alpha_1 U_3' - (r + U_1)(1 + U_1')\alpha_3) \, dr, \quad (6.6)$$

$$= \int_0^1 (h_0 \tilde{a}_1(\underline{U}; \underline{\alpha})_\Omega - P \tilde{a}_2(\underline{U}; \underline{\alpha})_\Omega) r \, dr \quad (6.7)$$

where, in the above, we have used integration by parts and made use of (3.28) and (3.34). In the case of  $J_2$  we have

$$\lambda'_3(\underline{U}; \underline{\alpha}) = -\lambda_3^2 \left( \lambda_1 \frac{\alpha_1}{r} + \lambda_2 \left( \frac{1 + U_1'}{\lambda_1} \alpha_1' + \frac{U_3'}{\lambda_1} \alpha_3' \right) \right). \quad (6.8)$$

Thus

$$J'_2(\underline{U}; \underline{\alpha}) = \frac{2}{b^2} \int_0^b (\underline{\alpha} \cdot J_\alpha(t, T) + \underline{\alpha}' \cdot J_{\alpha'}(t, T)) r \, dr \quad (6.9)$$

with

$$\underline{J}_\alpha(r, T) = -\frac{2\lambda_3^2}{b^2} \begin{pmatrix} \lambda_1/r \\ 0 \end{pmatrix}, \quad \underline{J}_{\alpha'}(r, T) = -\frac{2\lambda_3^2 \lambda_2}{b^2 \lambda_1} \begin{pmatrix} 1 + U_1' \\ U_3' \end{pmatrix}. \quad (6.10)$$

In the computations we use piecewise polynomials of one degree higher when approximately solving the dual problem for  $\underline{\psi}$  compared to those used to solve the problem for the approximate primal solution  $\underline{u} = \underline{u}_h$ . The approximation obtained with a uniform mesh of 1024 quadratic elements is sufficiently accurate here to be used as the “exact solution” in the computation of the error when we compare with the estimate of the error using the dual solution  $\underline{\psi} = \underline{\psi}_h$ . With this set-up everything works very well and the estimate  $-a(\underline{u}_h, \underline{\psi}_h)_\Omega$  of the error  $\bar{J}(\underline{U}) - J(\underline{u})$  is asymptotically exact and the adaptive refinement procedure quickly generates an approximation of a desired accuracy. This is illustrated in tables 6.1 and 6.2 for  $J_1(\underline{U})$  and in tables 6.3 and 6.4 for  $J_2(\underline{U})$ .

## 6.2 The dynamic problem – modelling error

The quasi-static displacement  $\underline{U}$  for the hyperelastic material at a given pressure only depends on the magnitude of that pressure, i.e. it does not depend on how rapidly the pressure is being applied, and it gives the solution to the dynamic problem when the pressure is applied infinitely slowly. This suggests that it is likely to be an accurate modelling assumption when the pressure is applied slowly but less accurate when the pressure is applied more rapidly. An obvious modelling question is then *how slow does the inflation process need to be for a given a quasi-static solution to be a good approximation to the true physics for a given  $QoI$ ?* A related

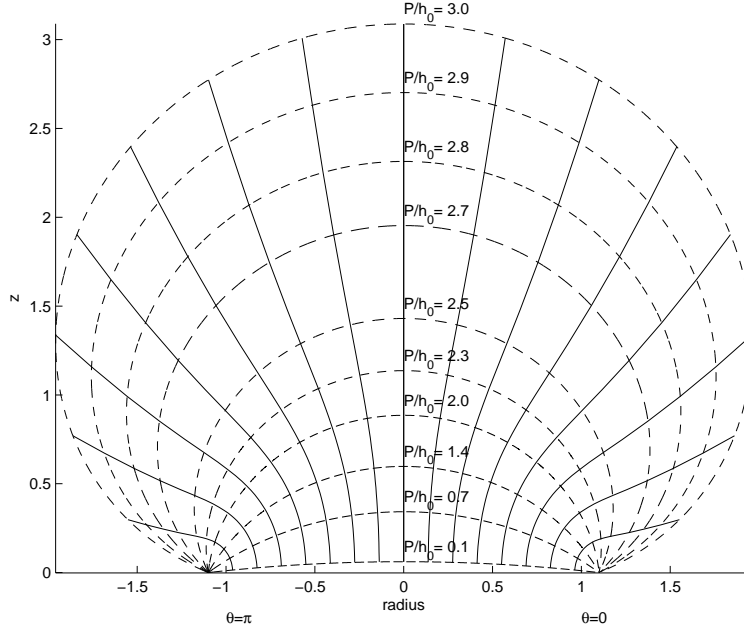


FIG. 6.1. Deformed profiles (dashed lines) and paths of points (solid lines) with the quasi-static model. The inflation starts after a uniform prestretch of magnitude 1.1.

question is concerned with *how good is the estimate*

$$J\left(\begin{pmatrix} U \\ V \end{pmatrix}\right) - J\left(\begin{pmatrix} \underline{u}_h \\ \underline{v}_h \end{pmatrix}\right) \approx F\left(\begin{pmatrix} \underline{\psi}_h \\ \underline{\theta}_h \end{pmatrix}\right) - A\left(\begin{pmatrix} \underline{u}_h \\ \underline{v}_h \end{pmatrix}; \begin{pmatrix} \underline{\psi}_h \\ \underline{\theta}_h \end{pmatrix}\right) \quad ? \quad (6.11)$$

For the axisymmetric inflation problem we are fortunate in that it is not too computationally expensive to approximately solve the full dynamic problem to test the performance of the estimate (although in other modelling situations this may be an expensive computation if a fine space mesh and a large number of time steps are required). It must of course not be overlooked that to obtain the error estimate we need to obtain  $\underline{\psi}_h$  and  $\underline{\theta}_h$  by solving a dual problem which, although linear, is a space time problem which may also need a fine mesh and a large number of time steps.

We consider the same inflation problem as in section 6.1 with the same material. The undeformed radius of the sheet is again 1, the initial thickness is now taken as  $h_0 = 10^{-2}$  and the density of the incompressible material is taken as  $\rho = 1$ . Before the inflation is started we prestretch the sheet so that  $U_1(1) = 0.1$ . The sheet is then clamped at its edge and then a time dependent pressure  $P(t)$  is applied where

$$P(t) = \frac{0.03t}{T}, \quad 0 \leq t \leq T. \quad (6.12)$$

The final pressure is thus  $P(T) = 0.03$  so that  $P(T)/h_0 = 3$  which corresponds to the largest forcing action used in figure 6.1 in the quasi-static inflation case. For the dynamic problem we

also need the initial velocity and this is set here as the velocity that the quasi-static solution gives at  $t = 0$  so that there is no difference between the quasi-static and dynamic cases at this stage.

In the following we consider the deformation that is obtained at different final times  $T$  corresponding to the different values for the rate

$$\tilde{\eta} = \frac{0.03}{T} \quad (6.13)$$

for two different QoI. With  $\eta = 100\tilde{\eta}$ , the rates that are considered are as follows:  $\eta = 0$  (quasi-static case),  $\eta = 2$ ,  $\eta = 4$ ,  $\eta = 6$ ,  $\eta = 9$ ,  $\eta = 20$ ,  $\eta = 80$ . The final deformation at these rates are shown in figure 6.2 and they show that there is a large difference between the profiles at the rates considered and hence there is a large difference between the final thickness (i.e. the thickness at time  $t = T$ ) in these cases. We consider the following two quantities of interest concerned respectively with thickness and with kinetic energy.

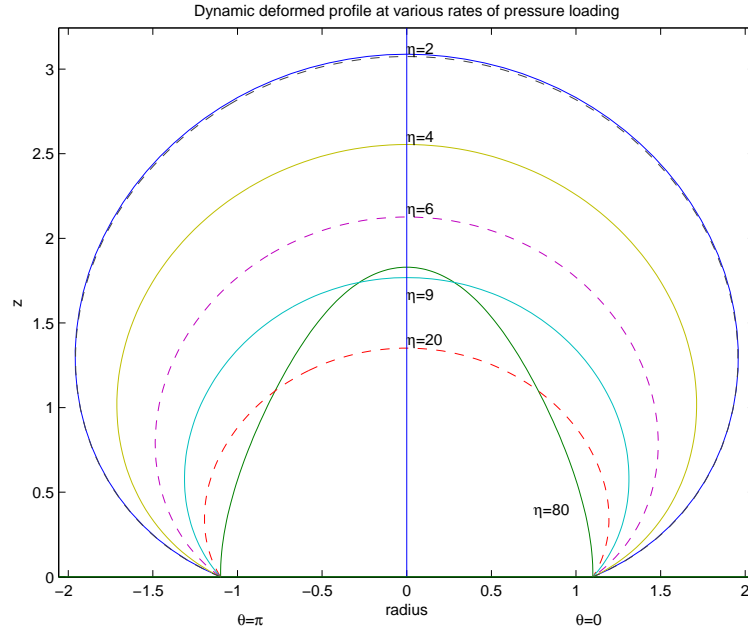


FIG. 6.2. Deformation at the final times  $T = 3/\eta$  (corresponding to the pressure  $P(T) = 0.03$ ) for  $\eta = 2$ ,  $\eta = 4$ ,  $\eta = 6$ ,  $\eta = 9$ ,  $\eta = 20$  and  $\eta = 80$ . The outermost curve is the slowest rate, the inner ‘parabolically-shaped’ curve is the fastest rate.

A kinetic energy type term close to the pole and near the final time Specifically we take

$$J_3(\underline{V}) = \frac{1}{2} \int_{0.9T}^T \int_0^b r \|\underline{V}\|^2 dr dt, \quad \text{with } b = 0.25. \quad (6.14)$$

In this case the Gâteaux derivative is simply

$$J'_3(\underline{V}; \underline{\beta}) = \int_{0.9T}^T \int_0^b \underline{\beta} \cdot \underline{J}_\beta(r, t) r dr dt, \quad \text{where } \underline{J}_\beta(r, t) = \begin{pmatrix} V_1 \\ V_3 \end{pmatrix}. \quad (6.15)$$

An average thickness near the pole at  $t = T$  We take

$$J_4(\underline{U}) = \frac{1}{\delta} \int_0^b r \lambda_3(r, T) dr, \quad \delta = \int_0^b r dr, \quad b = 0.25 \text{ in the example.} \quad (6.16)$$

The Gâteaux derivative here is

$$J'_4(\underline{U}; \underline{\alpha}) = \int_0^b (\underline{\alpha} \cdot \underline{J}_\alpha(r, T) + \underline{\alpha}' \cdot \underline{J}_{\alpha'}(r, T)) r dr \quad (6.17)$$

with  $\underline{J}_\alpha(r, T)$  and  $\underline{J}_{\alpha'}(r, T)$  being the same expressions as in (6.10).

In table 6.5 we show the predictions for  $J_3(\underline{V})$  obtained by solving the fine problem, obtained by just solving the coarse problem (i.e. solving the quasi-static problem for the displacement and then recovering the velocity) together with the actual error and the prediction of the error. In this case the error prediction is quite good throughout even when the difference between the quasi-static and dynamic membrane profiles is large. The good prediction throughout seems to be connected to a dual solution which is ‘fairly simple’ in that it is not highly oscillatory in space or time. In figures 6.3, 6.4 and 6.5 we show graphs of the profiles of  $\psi_1$  and  $\psi_3$  at the times  $2T/3$ ,  $T/3$  and 0 respectively. In this case as  $J_3(\underline{V})$  does not involve final time values we have  $\underline{\psi}(r, T) = \underline{\vartheta}(r, T) = \underline{0}$ ,  $0 \leq r \leq 1$ .

In table 6.6 we show the predictions for  $J_4(\underline{U})$  corresponding to the different rates at which the pressure is applied. In this case the coarse solution prediction (i.e. the quasi-static solution prediction) is the same in each case and hence the error is the difference between each value and 0.0478. The error prediction is that obtained using the solution of the dual problem. When the rate is low the prediction and the actual error agree quite well (see the rate  $1 \times 10^{-2}$ ) as the theory predicts whilst for the faster rates the prediction gives the correct order of magnitude but it is not a sharp estimate. This is about as much as can be expected as the theory only says that the estimate is good when the coarse solution is close to the fine problem. To get the error estimate we have to compute the dual solution which we find in this example is highly oscillatory in both space and time. Graphs of the profiles of  $\psi_1$  and  $\psi_3$  at the times  $2T/3$ ,  $T/3$  and 0 and corresponding to the fastest inflation rate are shown in figures 6.6, 6.7 and 6.8. The final time value of  $\underline{\psi}(r, T) = \underline{0}$  in this case but we have  $\underline{\vartheta}(r, T) \neq \underline{0}$  because  $J_4$  involves final time values. Similar profiles are obtained with all the other rates.

In all the computations given the coarse solution was obtained using  $\tilde{M} = 20$  quadratic elements and  $N = 200$  time steps. The dual solution was obtained with 40 quadratic elements and 400 time steps. This seems to be enough (and possibly more than enough) to ensure that the numbers given in the tables here are about accurate to all the digits given. To support this claim we give in table 6.7 values for the actual error and the prediction of this error for the inflation rate of  $4 \times 10^{-2}$  obtained using a different number of space elements and a different number of time steps. The closeness of the numbers in each column suggests that the space and time meshes are fine enough and that the error in estimating the QoI in each case is predominantly just the modelling error. The smoothness of the deformed profiles in figure 6.2



and also the results in table 6.5 indicate that not too many quadratic elements are needed for high accuracy but that a much larger number of time steps are needed to get a sufficiently accurate solution to the fine problem and indeed to the dual problem in some cases (e.g. the case of predicting  $J_4(\underline{U})$ ).

## 7. Conclusions

From the results presented in section 6 the technique of setting-up and solving a dual problem in order to generate an estimate of the error in a quantity of interest is we believe a qualified success in the context of membrane inflation. As the derivation suggested, and as we might expect, the technique does better, in the sense of accuracy of the estimate, the closer the coarse solution is to the unknown fine solution. In the simpler cases when we only have discretization error the technique also helps us adaptively to refine the space mesh to achieve (1.6). For more general and more difficult problems we will not have this case, as modelling error will also be involved and we no longer have convergence. We will have modelling error when, for example, the fine problem is very complicated and also needs a prohibitive amount of computation to approximately solve. (This is not the situation with the model considered in this paper in which we have a membrane assumption and axisymmetric geometry.) When we obtain a solution to one problem by solving a different (hopefully nearby) problem it is not clear in advance how good the approximation will be and what this paper demonstrates is that the technique ‘may’ be able to answer the question. We say ‘may’ as the success or otherwise depends on several factors.

- (i) When the computational cost of solving the linear dual problem is as much as that of attempting to solve the fine problem then there may not be too much of a gain unless the dual solution can help in the choice of the meshes in the coarse problem. This is what was done in the first example in section 6 when there was only discretization error.
- (ii) When the form of  $J(\cdot)$  leads to a dual solution that has complicated features and a fine space/time mesh is needed to resolve these features, then the gain may not be great as the cost of solving the dual problem adequately is high. It is not clear in advance for what forms for  $J(\cdot)$  this will be the case. In the examples presented above, the case  $J = J_3$ , involving kinetic energy, the components  $\psi_1$  and  $\psi_3$  do not contain any highly oscillatory features and the prediction of  $J(U) - J(u)$  is reasonable even when  $U$  and  $u$  are far apart. In contrast, in the case  $J = J_4$ , involving thickness, the components of the dual solution are highly oscillatory and the prediction is only good when  $U$  and  $u$  are close.

We hope to have demonstrated here that there are some hurdles to overcome in applying this technique. We need appropriate expressions for  $A'(\cdot; \cdot, \cdot)$  and  $J'(\cdot; \cdot)$ , although these only need to be determined once. A more significant obstacle is that the dual solution is solved using one mesh using data, the coarse solution, which is defined on a different mesh. This presents a stern challenge for most standard finite element libraries and packages, and makes the generation of bespoke code challenging.

To summarise, the success or otherwise of the technique used in this paper for estimating error is highly problem dependent. Whether or not it becomes more widely used a tool for

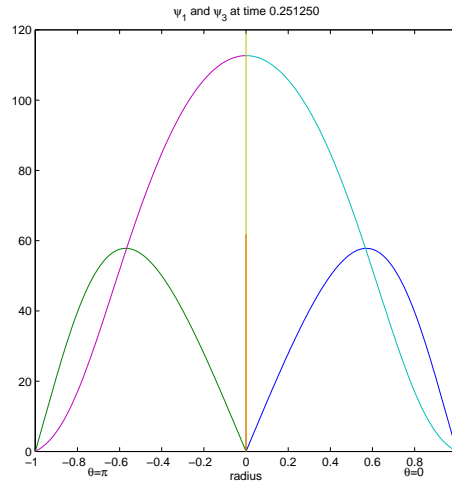


FIG. 6.3. Graphs of  $\psi_1(\cdot, 2T/3)$  and  $\psi_3(\cdot, 2T/3)$  at the fastest rate for  $J_3$ .

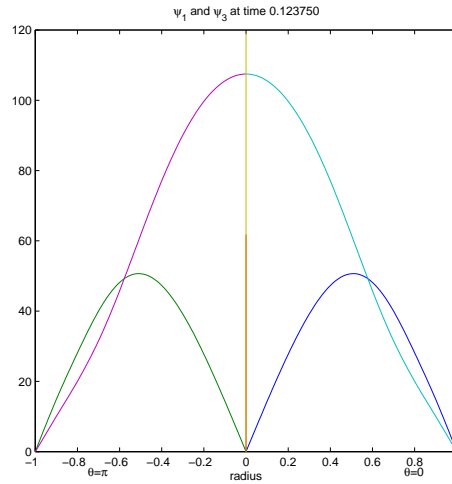


FIG. 6.4. Graphs of  $\psi_1(\cdot, T/3)$  and  $\psi_3(\cdot, T/3)$  at the fastest rate for  $J_3$ .

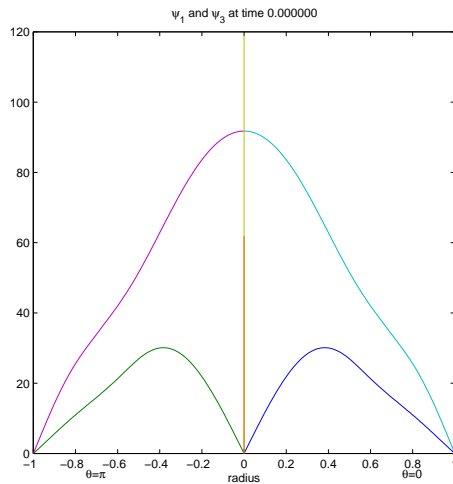


FIG. 6.5. Graphs of  $\psi_1(\cdot, 0)$  and  $\psi_3(\cdot, 0)$  at the fastest rate for  $J_3$ .

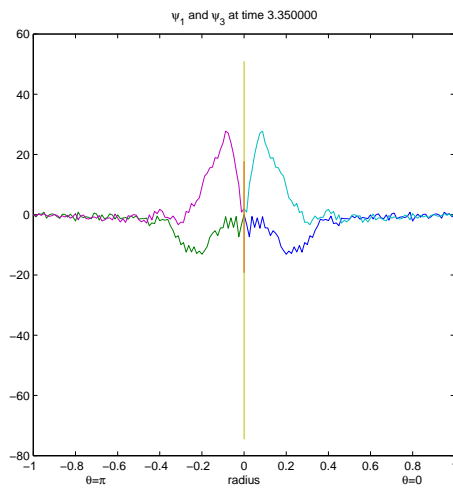
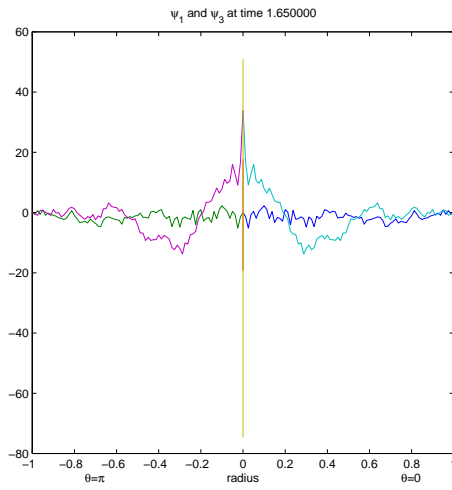
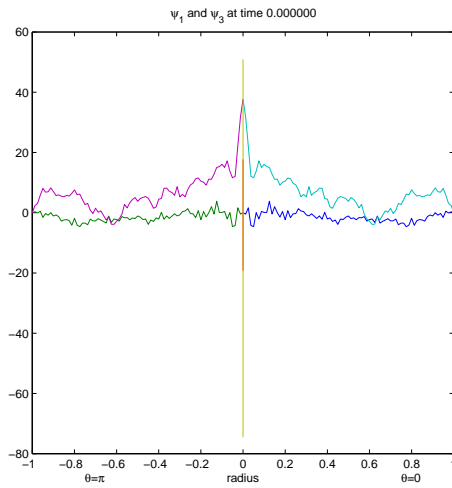


FIG. 6.6. Graphs of  $\psi_1(\cdot, 2T/3)$  and  $\psi_3(\cdot, 2T/3)$  at the fastest rate for  $J_4$ .

FIG. 6.7. Graphs of  $\psi_1(\cdot, T/3)$  and  $\psi_3(\cdot, T/3)$  at the fastest rate for  $J_4$ .FIG. 6.8. Graphs of  $\psi_1(\cdot, 0)$  and  $\psi_3(\cdot, 0)$  at the fastest rate for  $J_4$ .

assessing the reliability of engineering computations seems to depend on whether some form of *a priori* assessment of *its own reliability* becomes available, as well as on whether codes evolve to cope with the inherent complexity of the implementation.

### Acknowledgement

The authors would like to acknowledge the financial support of the US Army Research Office under grant W911NF-04-1-0185. They also wish to thank Dr. A.R. Johnson at the US Army Research Labs, Vehicle Technology Directorate, Hampton, VA for collaborating on this work.

### REFERENCES

- [1] Mark Ainsworth and J. Tinsley Oden. *A posteriori error estimation in finite element analysis*. Pure and applied mathematics. New York: Wiley, 2000.
- [2] H. Andrä, M. K. Warby, and J. R. Whiteman. Contact problems of hyperelastic membranes: Existence theory. *Math. Meth. Appl. Sci.*, 23:865–895, 2000.
- [3] I. Babuška, F. Nobile, and R. Tempone. Reliability of computational science. *Num. Methods for PDEs*, 23/4:753–784, 2007.
- [4] Ivo Babuška and Theofanis Strouboulis. *The Finite Element Method and its Reliability*. Numerical Mathematics and Scientific Computation. Oxford University Press, 2001.
- [5] Wolfgang Bangerth and Rolf Rannacher. Finite element approximation of the acoustic wave equation: Error estimation and mesh adaptation. *East-West Journal of Numerical Mathematics*, (4):263–282, 1999.
- [6] M. Brifcani, M. K. Warby, and J. R. Whiteman. A new tool for the design of thermoforming polymeric structures. *British Plastics and Rubbers*, pages 4–8, 1994. July/August.
- [7] W. G. Jiang, M. K. Warby, J. R. Whiteman, S. Abbott, W. Shorter, P. Warwick, T. Wright, A. Munro, and B. Munro. Finite element modelling of high air pressure forming processes for polymer sheets. *Computational Mechanics*, (31):153–172, 2003.
- [8] M. Karamanou, M. K. Warby., and J. R. Whiteman. Computational modelling of thermoforming processes in the case of finite viscoelastic materials. *Comput. Methods Appl. Mech. Engrg.*, 195:5220–5238, 2006.
- [9] J. T. Oden and Serge Prudhomme. Adaptive modeling in computational mechanics. Technical report, 02-05, TICAM, University of Texas at Austin, 2002. [www.ices.utexas.edu/research/reports/2002/0205.pdf](http://www.ices.utexas.edu/research/reports/2002/0205.pdf).
- [10] J. T. Oden and K. Vemaganti. Estimation of local modeling error and goal-oriented adaptive modeling of heterogeneous materials; part i: Error estimates and adaptive algorithms. *J. Comp. Physics.*, 164:22–47, 2000.
- [11] J. Tinsley Oden, S. Prudhomme, D. C. Hammerand, and M. S. Kuczma. Modeling error and adaptivity in nonlinear continuum mechanics. *Computer Methods in Applied Mechanics and Engineering*, 190:6663–6684, 2001.
- [12] R. W. Ogden. *Non-linear elastic deformations*. Dover, New York, 1984.
- [13] Serge Prudhomme and J.T. Oden. Goal-oriented error estimation and adaptivity for the finite element method. *Computers & Mathematics with Applications*, 41:735–756, 2001.

Table 6.1. In this table  $P = 3$ , we are estimating  $J_1(\underline{U}) = -1.501627519302$ , we use linear elements and we perform adaptive refinement. The accuracy desired corresponds to  $\text{tol} = 10^{-7}$ .

Elements $m$	Error est. $-a(\underline{u}_h, \underline{\psi}_h)$	Asymptotic exactness $-a(\underline{u}_h, \underline{\psi}_h)/(J_1(\underline{U}) - J_1(\underline{u}_h)) - 1$
8	$-9.25 \times 10^{-2}$	$-7.9 \times 10^{-2}$
128	$-4.21 \times 10^{-4}$	$-2.6 \times 10^{-4}$
2030	$-1.65 \times 10^{-6}$	$-2.4 \times 10^{-7}$
9293	$-7.02 \times 10^{-8}$	$+1.8 \times 10^{-5}$

Table 6.2. In this table  $P = 3$ , we are estimating  $J_1(\underline{U})$ , we use quadratic elements and we perform adaptive refinement. The accuracy desired corresponds to  $\text{tol} = 10^{-10}$ .

Elements $m$	Error est. $-a(\underline{u}_h, \underline{\psi}_h)$	Asymptotic exactness $-a(\underline{u}_h, \underline{\psi}_h)/(J_1(\underline{U}) - J_1(\underline{u}_h)) - 1$
8	$-3.29 \times 10^{-4}$	$-4.0 \times 10^{-3}$
128	$-5.14 \times 10^{-9}$	$+2.3 \times 10^{-4}$
396	$-4.06 \times 10^{-11}$	$+3.1 \times 10^{-2}$

Table 6.3. In this table  $P = 3$ , we are estimating  $J_2(\underline{U}) = 0.046930267582$ , we use linear elements and we perform adaptive refinement. The accuracy desired corresponds to  $\text{tol} = 10^{-7}$ .

Elements $m$	Error est. $-a(\underline{u}_h, \hat{\underline{\psi}}_h)$	Asymptotic exactness $-a(\underline{u}_h, \hat{\underline{\psi}}_h)/(J_2(\underline{U}) - J_2(\underline{u}_h)) - 1$
8	$-1.46 \times 10^{-3}$	$-1.0 \times 10^{-1}$
128	$-6.70 \times 10^{-6}$	$-3.2 \times 10^{-4}$
1289	$-4.52 \times 10^{-8}$	$-7.1 \times 10^{-5}$

Table 6.4. In this table  $P = 3$ , we are estimating  $J_2(\underline{U})$ , we use quadratic elements and we perform adaptive refinement. The accuracy desired corresponds to  $\text{tol} = 10^{-10}$ .

Elements $m$	Error est. $-a(\underline{u}_h, \hat{\underline{\psi}}_h)$	Asymptotic exactness $-a(\underline{u}_h, \hat{\underline{\psi}}_h)/(J_2(\underline{U}) - J_2(\underline{u}_h)) - 1$
8	$-2.11 \times 10^{-5}$	$-2.33 \times 10^{-3}$
128	$-3.47 \times 10^{-10}$	$+2.5 \times 10^{-4}$
257	$-1.79 \times 10^{-11}$	$+4.9 \times 10^{-3}$

Table 6.5. Prediction of  $J_3(\underline{V})$  by solving the fine problem, by solving the coarse problem, the error in the prediction and the estimate of the error by solving obtained using the solution to the dual problem.

Rate $\times 10^{-2}$	Exact	Estimate	Error	Error Prediction
1	$4.04 \times 10^{-2}$	$4.37 \times 10^{-2}$	$3.32 \times 10^{-3}$	$3.10 \times 10^{-3}$
2	$8.07 \times 10^{-2}$	$1.02 \times 10^{-1}$	$2.10 \times 10^{-2}$	$1.94 \times 10^{-2}$
3	$1.21 \times 10^{-1}$	$1.19 \times 10^{-1}$	$-2.45 \times 10^{-3}$	$4.03 \times 10^{-3}$
4	$1.61 \times 10^{-1}$	$1.02 \times 10^{-1}$	$-5.98 \times 10^{-2}$	$-5.33 \times 10^{-2}$
5	$2.02 \times 10^{-1}$	$8.12 \times 10^{-2}$	$-1.21 \times 10^{-1}$	$-1.23 \times 10^{-1}$
10	$4.03 \times 10^{-1}$	$4.53 \times 10^{-2}$	$-3.58 \times 10^{-1}$	$-4.98 \times 10^{-1}$
20	$8.07 \times 10^{-1}$	$1.12 \times 10^{-2}$	$-7.96 \times 10^{-1}$	$-1.40 \times 10^{+0}$
40	$1.61 \times 10^{+0}$	$2.74 \times 10^{-2}$	$-1.59 \times 10^{+0}$	$-2.81 \times 10^{+0}$
80	$3.23 \times 10^{+0}$	$5.74 \times 10^{-2}$	$-3.17 \times 10^{+0}$	$-5.66 \times 10^{+0}$

Table 6.6. The estimate of  $J_4(\underline{U})$  by solving the fine problem, the error by predicting using the coarse problem and the estimate of the error computed using the dual solution.

Rate $\times 10^{-2}$	Estimate	Error	Error Prediction
0	$4.782 \times 10^{-2}$	-	-
1	$4.767 \times 10^{-2}$	$-1.477 \times 10^{-4}$	$-1.406 \times 10^{-4}$
2	$4.782 \times 10^{-2}$	$7.329 \times 10^{-6}$	$-1.956 \times 10^{-4}$
3	$5.323 \times 10^{-2}$	$5.409 \times 10^{-3}$	$3.647 \times 10^{-3}$
4	$6.070 \times 10^{-2}$	$1.288 \times 10^{-2}$	$8.168 \times 10^{-3}$
5	$7.405 \times 10^{-2}$	$2.623 \times 10^{-2}$	$1.338 \times 10^{-2}$
10	$1.438 \times 10^{-1}$	$9.605 \times 10^{-2}$	$3.127 \times 10^{-2}$
20	$1.775 \times 10^{-1}$	$1.297 \times 10^{-1}$	$4.217 \times 10^{-2}$
40	$2.270 \times 10^{-1}$	$1.792 \times 10^{-1}$	$4.819 \times 10^{-2}$
80	$4.399 \times 10^{-1}$	$3.921 \times 10^{-1}$	$6.511 \times 10^{-2}$

Table 6.7. The ‘actual error’ and the prediction of the error using the dual solution using different numbers of quadratic space elements and time steps in the case of the inflation rate of  $4 \times 10^{-2}$ .

		Thickness QoI		K.E. QoI	
ne	nt	Actual error	Prediction	Actual error	prediction
20	100	$1.284 \times 10^{-2}$	$7.783 \times 10^{-3}$	$-5.960 \times 10^{-2}$	$-5.440 \times 10^{-2}$
20	200	$1.287 \times 10^{-2}$	$8.165 \times 10^{-3}$	$-5.971 \times 10^{-2}$	$-5.324 \times 10^{-2}$
40	200	$1.287 \times 10^{-2}$	$8.165 \times 10^{-3}$	$-5.974 \times 10^{-2}$	$-5.326 \times 10^{-2}$
40	400	$1.289 \times 10^{-2}$	$8.169 \times 10^{-3}$	$-5.976 \times 10^{-2}$	$-5.329 \times 10^{-2}$